Journal of Hydrology 627 (2023) 130358

Contents lists available at ScienceDirect

Journal of Hydrology

journal homepage: www.elsevier.com/locate/jhydrol

Research papers

Intercomparison of marine tracer and catchment-based submarine groundwater discharge estimates for a karst aquifer

Maxime Savatier[a,*], Patrick Morrissey[b], Laurence Gill[b], Carlos Rocha[c,*]

[a] Direction Scientifique et Technique, Centre de Meuse Haute Marne, Agence Nationale pour la gestion des Déchets Radioactifs, Bure, France
[b] Department of Civil, Structural and Environmental Engineering, Trinity College Dublin, Dublin 2, Ireland
[c] Biogeochemistry Research Group, School of Natural Sciences, Trinity College Dublin, Dublin 2, Ireland

A B S T R A C T

Submarine groundwater discharge (SGD) is a major source of solutes to the ocean. Consequently, the accuracy of estimates of the magnitude and seasonal variability of SGD is critical for the management of coastal marine ecosystems. However, very few intercomparison studies between different conceptual approaches have been made to assess the reliability and consistency of SGD flow estimates while simultaneously gauging the applicability of underlying models and budget assumptions in real-world scenarios. To date, intercomparison efforts have focused on homogeneous aquifers, and less so on highly heterogeneous aquifers such as karst systems. Here we compare the results of tracer-based (salt mass balance, tidal prism and radon mass balances) and catchment-based methods (water balance, semi-distributed karst network model) to assess SGD at a data-rich coastal location. All approaches tested here reveal a positive relationship between SGD fluxes and groundwater level measured close to the preferential groundwater flow pathways in the phreatic karst aquifer (e.g. water-saturated conduits or fracture network). We use this finding to derive site-specific relationships between groundwater level and SGD flow rates. We derive these relationships from least square fitting of Darcian and Non-Darcian models and regression analysis. The relationships validate the findings derived independently from hydraulic/hydrogeological modelling of the complex karst networks. By combining various estimates made with distinct assumptions, this method produces robust estimates of the SGD seasonal variability, essential to develop optimal management strategies of SGD resources in coastal karstic regions. Where direct measurements of SGD are not possible, monitoring of coastal groundwater level close to preferential phreatic groundwater pathways can be thus used as a useful indicator to compare past groundwater flow measurements and derive site-specific relationships, particularly in settings where large flow rate changes are present such as karst aquifers.

1. Introduction

Submarine Groundwater Discharge (SGD) is a crucial source of dissolved chemicals to coastal areas and the global ocean, and may play a larger role in oceanic nutrient budgets than river water (Kwon et al., 2014; Moore et al., 2008; Santos et al., 2021). Protecting coastal ecosystem value for humankind requires reliable estimates of SGD rates to (1) assess the effect of SGD fluxes on salinity and water chemistry to maintain healthy coastal ecosystems, and (2) validate marine biogeochemical budgets of elements such as carbon, nitrogen and phosphorus. SGD comprises fresh groundwater fluxes driven by rainfall recharge on land and seawater recycled through coastal aquifers and sediment at various temporal and spatial scales (Burnett et al., 2003). Similarly, in coastal karst aquifers, water fluxes are driven by aquifer recharge, saline intrusion through conduits connected to the sea, or both (Fleury et al., 2007).

In this context, hydrogeologists and oceanographers tend to approach the same problem from different directions. Standard hydrological approaches include measurement of the hydraulic gradient on land with flow estimated either analytically or numerically (Burnett et al., 2006; Gill et al., 2013). On the other hand, oceanographers have been using seepage meters, mini-piezometers and geochemical tracers to estimate SGD in the coastal zone (Burnett et al., 2006; Taniguchi et al., 2019). However, each method has inherent uncertainties, which are sometimes larger than the fluxes being assessed (Burnett et al., 2001). Intercalibration experiments are therefore necessary to compare the existing methods employed in deriving SGD rates to build confidence in their accuracy (Burnett et al., 2001). A series of studies have combined marine tracers and hydrogeology to assess SGD fluxes in homogenous media such as sands and quaternary aquifers (Burnett et al., 2008; Mulligan and Charette, 2006; Smith and Zawadzki, 2003), or in heterogeneous media such as karst aquifers (e.g. Mejías et al., 2012; Montiel et al., 2018; Smith and Zawadzki, 2003) or fractured aquifers (Burnett et al., 2008). Most, if not all studies combine various methods to assess SGD focused at specific times of the year (e.g Burnett et al., 2002, 2008; Dulaiova et al., 2006; Smith and Zawadzki, 2003), localised springs (Mejías et al., 2012; Montiel et al., 2018; Smith and Zawadzki, 2003) or to give a first assessment of the magnitude of SGD fluxes during

* Corresponding authors.
E-mail addresses: maxime.savatier@andra.fr (M. Savatier), rochac@tcd.ie (C. Rocha).

https://doi.org/10.1016/j.jhydrol.2023.130358
Received 25 July 2023; Received in revised form 3 October 2023; Accepted 5 October 2023
Available online 23 October 2023

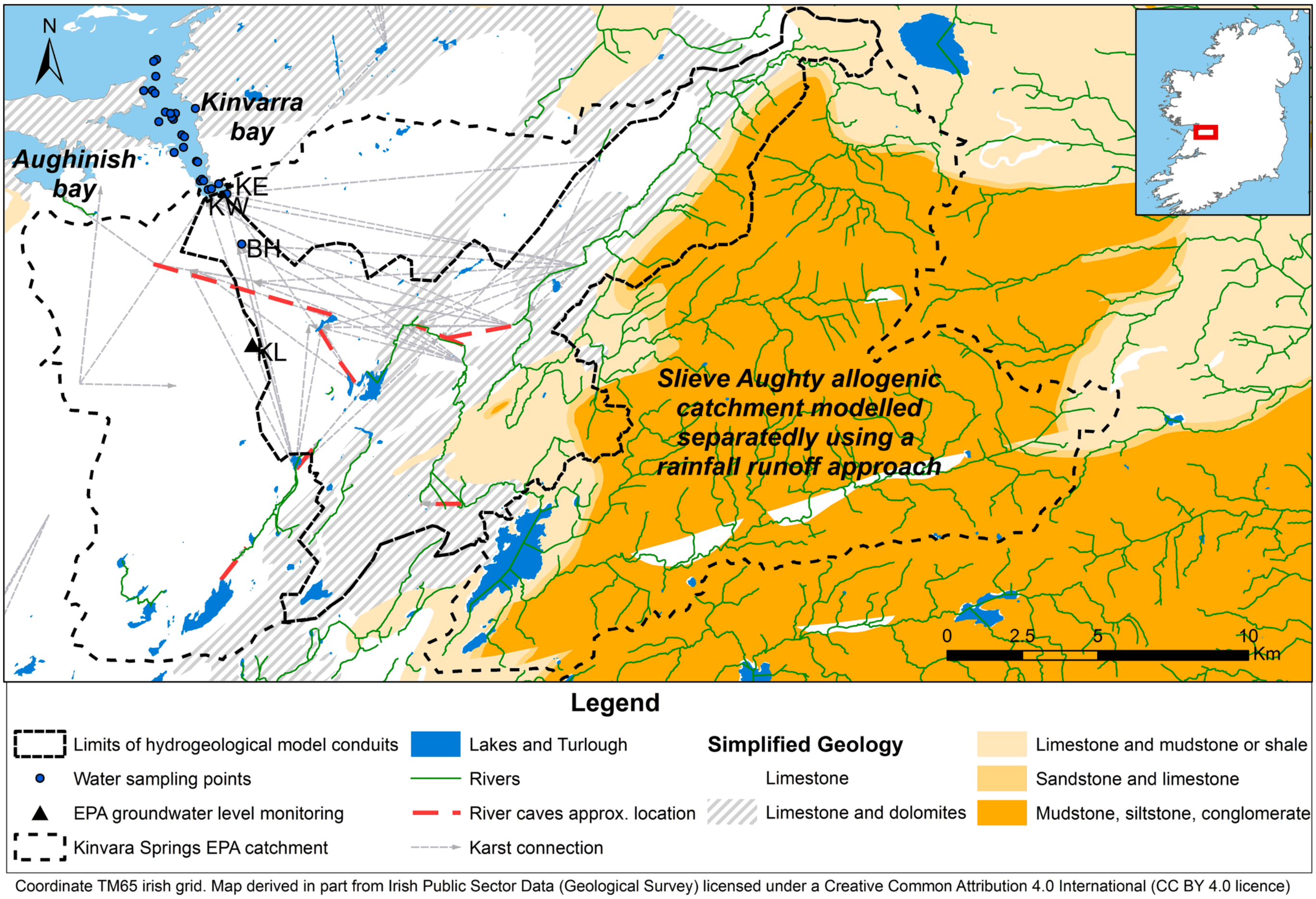

Fig. 1. Kinvarra bay and the catchment of Kinvarra springs, with the boundary of the pipe network hydrogeological model, and the limits of the upper catchment sections modelled with a rainfall-runoff approach. Kinvarra West/Arch (KW) and Kinvarra East/Castle (KE) are the two main springs of the bay. BH is a borehole located close to the main conduit feeding Kinvarra springs and sampled in this study. The EPA monitor groundwater level continuously at Killiny Borehole (KL). Geology (Geological Survey, 2019) is grouped by main lithologies relevant for water circulation within the catchment. Grey dotted lines connect locations linked by a karst network, as identified by tracing studies (Geological Survey, 2019). The red dashed lines are the approximate location of major cave network (e.g.: underground river) identified by surface features and cave exploration (Drew, 2003), modified following maps of Morrissey et al., (2020). Three rivers flowing off the Slieve Aughty mountains providing allogenic input to the lowlands are modelled separately using a rainfall runoff approach. (For interpretation of the references to colour in this figure legend, the reader is referred to the web version of this article.)

specific periods (most previous references). Few studies so far have characterised the full variability of SGD during the year resulting from the change of gradient between sea level and groundwater level.

Early intercalibration experiments were done in settings where groundwater levels were relatively stable during the year (e.g. $\pm$ 1 m in Giblin and Gaines, 1990 or in Mulligan and Charette, 2006). As a result, they frequently compared estimates made at different times and groundwater levels, assuming similar flow conditions. Karst systems and fractured aquifers, however, generally show larger changes of groundwater head than homogenous aquifers, which would translate into higher fluctuations of the magnitude and composition of SGD fluxes during the year. For example, submarine or coastal karst springs reviewed by Fleury et al. (2007) have their discharge multiplied by a factor of 3 to 300 from dry to wet periods. Inter-alia, this variability was noted in the intercomparison of Montiel et al., (2018), but limited to a comparison between “wet” and “dry” periods. Annual average flow rates of submarine karst springs also vary substantially between sites, with flow from point source springs ranging from 0.01 to 300 m^3/s (Fleury et al., 2007; Paloc and Potie, 1974; Williams, 1974). Flows from karst springs vary strongly with the head difference between the karst network feeding the spring and the level of the water body receiving its flow (here the sea), and may also receive saline inputs in systems where deep karst conduits connected to the sea or deep saline aquifers are present (Fleury et al., 2007; Paloc and Potie, 1974). Despite this known variability, studies going beyond providing more than point source estimates of flow rates from karstic submarine spring to estimate flow rates over long periods remain rare, limiting the understanding of karstic aquifer systems with submarine outlets (Fleury et al., 2007) and their effects on marine chemistry and ecology (e.g. Bejannin et al., 2020). Direct measurements of discharge from submarine conduit flows are not always technically feasible or logistically practical, and often do not allow quantification of the totality of water fluxes crossing the subsurface land-sea boundary, over a wide range of space and timescale (Fleury et al., 2007; Taniguchi et al., 2019). Tracer-based methods allow such quantifications to be made, if compositions of the end members are well characterized (Fleury et al., 2007; Povinec and Aggarwal, 2006; Rocha et al., 2016). Recent studies in Ireland have also used measurement of groundwater-surface water interactions in ephemeral karst lakes (known as turloughs in Ireland) combined with salt budgets to develop and validate hydrogeological models for marine systems connected to karst aquifers (Gill et al., 2013; McCormack et al., 2016; Morrissey et al., 2020). A combination of tracers, including radon and stable isotopes of water, were also used to assess discharge in the same system (McCormack et al., 2016; Rocha et al., 2015; Schubert et al., 2015). The question remains, however, as to how the different estimates derived using such distinct methods compare across different recharge conditions. To our knowledge, no intercomparison experiments has yet been carried out with this specific aim, either in Ireland or abroad.

In this context, Kinvarra bay is a well-suited test site to assess the seasonal variability of SGD fluxes because the majority of its freshwater inputs comprise groundwater originating from an extensive and well-studied karst hinterland. We combine results from hydrogeological modelling (Morrissey et al., 2020), tracer based methods (Cave and Henry, 2011; Rocha et al., 2015; Savatier and Rocha, 2021; Schubert et al., 2015) and direct discharge measurements on specific springs in conduits connected to this bay (Drew, 2008). To allow a comparison between flow estimates made at different time periods, we correlate this data with the groundwater level measured (with reference to a variable sea level) in a location hydraulically connected to the main karst conduit feeding Kinvarra spring. This intercomparison exercise evaluates the effect of the annual variability of groundwater level on SGD rates. We then derive site specific relationships between fresh SGD and groundwater level, providing a method which may be valuable in other sites receiving fluxes from karst aquifers to estimate the effect of groundwater head relative to sea level on groundwater discharge. This can provide useful information to support appropriate water management in such sites.

2. Material and methods

2.1. Site description

Kinvarra Bay in the west coast of Ireland is connected to a major karst network (Fig. 1). The bay receives major inputs of groundwater (with discharge estimates ranging between 0.2- to above 30 m^3s^{-1} according to the review of Savatier and Rocha, 2020), mainly from two springs located in the upper part of the bay, Kinvarra East (Castle) and Kinvarra West (Arch). Some potential additional springs were also identified at Tarea Pier (Schubert et al., 2015). The Kinvarra West/Arch spring is fed from a catchment estimated to be between 483 km^2 (EPA, 2011) and 500 km^2 (Morrissey et al., 2020; Naughton et al., 2018), with a lower part of well-developed limestone karst system, served in part by river water coming from an upper catchment of old-red sandstone (Clare and Mcnamara, 2009) (Fig. 1). The catchment area for the Kinvarra East/Castle spring has been estimated to be 88 km^2(McCormack et al., 2014). According to Cave and Henry, (2011), the Arch spring tends to dry during droughts, while the Castle spring is active at low tide even during extended summer drought, which may suggest a deeper pathway of the water flowing to the Castle spring. Analysis of trace elements in the two springs showed that the system feeding the Arch springs contains autogenic water (coming from infiltrated rainfall directly onto the karst catchment to the east) compared to the castle spring which contains a mix of autogenic recharge and allogenic recharge from the Sleive Aughty mountains to the south which discharge down into the extensive karst conduit network (Gill et al., 2018). However, some tracer studies have showed that there may be a small high level connection between the two karst catchments at very high groundwater levels (Drew, 2003; Gill et al., 2018) (Karst connections, Fig. 1). The EPA monitors groundwater level at Killiny Borehole (KL, Fig. 1) and quality at Loughcurra South (BH, Fig. 1), which is close to the main series of conduits feeding Kinvarra East and West. Kinvarra East and West do not have distinct radon or stable isotope signatures during summer (Schubert et al., 2015).

2.2. Tracer-based methods

Tracer-based methods to detect SGD locations and quantify SGD fluxes use the measurement of elements whose concentration changes relative to seawater as a result of SGD (e.g., for total SGD: radon, radium, stable isotopes, methane or silicon) (Burnett et al., 2006). The quantification of SGD fluxes with the tracer methods requires an evaluation of any other sources of the tracer and an "end member" concentration to be chosen that is representative of SGD.

Savatier and Rocha (2020) reviewed previous estimates of discharge from Kinvarra spring and assessed different methods to estimate SGD from conservative (e.g., salinity) and non-conservative tracers (generally subject to time dependant losses that can be quantified, such as decay, e.g. ^{223}Ra, ^{224}Ra, ^{222}Rn or degassing e.g. ^{222}Rn). This study showed that SGD estimates based on single point time series (Eulerian) outside of a water retention area can lead to consistently lower estimates than when sampling tracers using transect data (Lagrangian). Moreover, it showed that the outcome of radon (^{222}Rn) based SGD estimates is dependent on how the effect of water age variability on radon decay and degassing is accounted for. On this basis, the study proposed a correction of ^{222}Rn budgetary approaches to estimate SGD, based on the spatial variation of water ages estimated from dissolved radium isotopes (^{223}Ra, ^{224}Ra).

Considering these findings, for the purpose of this study, we thus employ radon budgets based on longitudinal data, corrected for the effect of water ageing, following Savatier and Rocha, (2020).

Moreover, among the different types of tidal prism methods tested in Savatier and Rocha (2020), we select here those allowing for the return during the flood tide of water that left the bay during the previous ebb tide (Model C in Luketina, 1998 and the tidal prism method used in Eq. (2) in Cave and Henry, 2011) for two reasons. First, including a return flow is consistent with previous estimates by Rocha et al. (2015) of a return flow factor in the bay of 0.86 ± 0.04 during summer and recent further evidence of storage for several tidal cycles of freshwater in the inner bay by Gregory et al., (2020). Secondly, including return flow leads to discharge rates similar to previous estimates based on tracers, hydrogeological modelling or water balances. Discharge estimates from Guerra et al. (submitted, as cited in Savatier and Rocha, 2020) and from Cave and Henry (2011), which are derived from Eq. (2) in Cave and Henry (2011) are also included here as they consider return flow. Estimates from Eq. (1) in Cave and Henry (2011), did not account for return flow and led to freshwater inputs to the bay higher by one order of magnitude than other estimates and are thus not included here. Finally, for comparison purposes we also give the early flow estimates by Drew (2008); annual average fresh water inputs to the bay derived from water balance by Schubert et al. (2015); the single point estimate of the flow from Kinvarra East and West derived from the change of volume of the salt wedge within the bay (McCormack et al., 2016) and total SGD and freshwater inputs estimates from Rocha et al. (2015) based on radon and salt mass balances.

2.3. Hydrogeological model

A semi-distributed 1D model of the catchment was developed in the Infoworks ICM (Innovyse) urban drainage software to simulate groundwater-surface water interaction for 15 turloughs across the catchment, and floodplains (see Morrissey et al., 2020 for more details). This was based on a previous 1D semi-distributed model of the five turloughs due to its ability to model the hydraulics of the karst conduit network in both open channels and pressurised pipe flows (Gill et al., 2013a). The groundwater-surface water turlough dynamics were modelled as storage ponds in the software which were configured with the same depth-volume characteristics as the surface topography, as derived from the DEM. Diffuse recharge from rainfall is modelled per sub-catchment via a series of reservoirs: rainfall-runoff, soil, and groundwater stores in series, all yielding different delayed discharges in parallel into the pipe network. All flows discharge into permeable pipes, one connected for each sub-catchment to represent the primary and secondary permeability. The allogenic recharge into the karst network from the rivers flowing off mainly from the old red sandstone mountains was input as point flow time series into the head of the pipe network. These data were derived by three separate rainfall-runoff models (one for each river), using the MIKE11-NAM software (DHI Software). Certain key floodplains were also included as 2-D areas into the model to allow for overland flow between turloughs/floodplains which was not previously accounted for and therefore provided an accurate representation of flooding mechanisms across the whole catchment. The final 1-D/2-D model network was developed on the back of previous field investigations (tracer studies, caving records etc.), with further insights into the system gained from the accumulating hydro-meteorological data across the catchment as well as water hydrochemistry (Morrissey et al., 2020). Time and frequency series analyses on the continuous water level measurements of the five turloughs in the linked network were used in order to elucidate the nature of the hydraulic pipe configurations at key points in order to improve the conceptual model (Gill et al., 2013b; Morrissey et al., 2020).

2.4. Relationship between SGD estimates and groundwater table

As Kinvarra Bay hosts a series of submarine springs in a rocky shore setting, and flow occurs both in focused and diffuse manner, no direct measurement of the totality of flows is feasible on the site. Thus, to allow for an inter-annual comparison between different studies, we related the SGD estimates obtained in each study (Cave and Henry, 2011; Drew, 2008; Gill et al., 2013a; McCormack et al., 2016; Morrissey et al., 2020; Rocha et al., 2015; Schubert et al., 2015) to the groundwater level (taken from EPA dataset, 2020) that was present next to the main conduit feeding Kinvarra east and west, Killiny Borehole, at the time when each study estimated SGD rates.

We make this choice for the following reasons: SGD estimates for Kinvarra Bay using salinity (Cave and Henry, 2011; Rocha et al., 2015; Savatier and Rocha, 2021), radon (Rocha et al., 2015; Savatier and Rocha, 2021) and hydrogeological modelling (McCormack et al., 2014) are positively correlated with groundwater level measured at Killiny, as previously shown (Savatier and Rocha, 2021). Moreover, tracer tests and cave exploration showed that Killiny borehole is less than 1 km away from a series of conduits feeding Kinvarra springs (Boycott et al., 2003). Because flow rates in the conduit are estimated to vary between 60 and 1000 m h^{-1} (Drew, 2003), conduit flows would cross this distance in less than a day. This proximity, the hydrological connections, and the correlation observed between fresh SGD and groundwater level suggest that daily averaged groundwater level at Killiny borehole is a good indicator of the variability of hydraulic head in the conduit feeding Kinvarra spring, and thus of the fresh SGD coming to Kinvarra bay. It should be noted here that the level in Caherglassaun turlough, the most downstream turlough with several years of dataset available (Basu et al., 2022) might also have been used here to test the discharge-height relationship. Killiny borehole was preferred here as it has been monitored since 1995, and has continuous monitoring of level since October 2003, with updated level dataset publicly available online and continuing until present time (EPA, 2023), which provide a common reference to compare the height discharge relationship for the studies carried out over the last decade.

We fit a first-order relationship between groundwater level measured at Killiny and the daily averaged fresh SGD into Kinvarra bay using a regression analysis of the flow estimates derived by previous studies. When fitting a regression from a limited number of datapoints derived from different methods, which can be biased in different ways, the chosen relationship should ideally represent the physical driver of flows in a realistic manner, so as to limit overfitting with relationships lacking physical basis. Two types of such relationships can be derived: equations assuming that the flow in the aquifer is laminar, including the commonly used Darcy law (for flow in porous media) and the Hagen-Poiseuille equation (for flow in a conduit), or equations assuming turbulent flow conditions in the aquifer conduit. The two first expressions are used for discrete element modelling in FEFLOW (Diersch, 2009), or for conduit flow processing in MODFLOW (e.g. Shoemaker et al., 2008). Equations to assess turbulent flow in conduits generally require more information on conduit or fracture shape, length, roughness, or other physical parameters that are in practice challenging to characterise precisely from a flow measurement dataset. A classical approach to non-darcian turbulent flow in a network of karst conduits is the combination of the Darcy–Weisbach and the Colebrook-White equations (used for example for conduit flow processes in an updated version of MODFLOW (unstructured grid (USGS) with continuous linear network (CLN)) see Shoemaker et al., (2008) and Duran and Gill, (2021). In hydraulic/hydrological models (such as Infoworks ICM) these standard equations are frequently replaced by the Saint Venant equations of unsteady flow, to allow to model continuously variable flow conditions in time and space within distinct network shapes. These models, however, require information on conduit shape, tortuosity, length of conduit and mean surface roughness of the conduit. A recent alternative which does not require these data has been developed from the Torricelli formula (a derivation of the Bernoulli Law) based on the assumption that karst has fractal properties (Maramathas and Boudouvis, 2010). Porous or fractured media generally have characteristics of the fractals: self-similarity (Paredes and Elorza, 1999; Yu and Cheng, 2002), i.e. similar shapes are found at various scales.

Here we test these three options of the Darcy equation, the Darcy–Weisbach and Colebrook-White equation and the Fractal approximation, to assess their fit to the observed correlation between groundwater level and the tracer-based estimates of SGD. This analysis was carried out in two steps:

First, we fit the parameters of the three relationship types and assess their uncertainty using the non-linear least square fitting library of the open-source R software. Total SGD estimates are not directly comparable with estimates from hydrogeological models since they also include seawater recirculated through the coastal aquifer and are susceptible to non-steady variability of water ages and flushing in the bay when based on non-conservative tracers (Savatier and Rocha, 2021). To compare tracer based to model-based estimates of SGD, we thus focus our analysis on fresh-SGD estimates, using three alternative hypotheses.

Secondly, after adjusting the parameters of each relationship to the SGD estimates by regression, we compute the 95th % confidence and 95th % prediction intervals for each curve through higher order Taylor expansion and Monte Carlo simulation (using the propagate package in R statistical software, Spiess, 2018) and the tracer-based estimates of flow coming to Kinvarra Bay.

We detail further below how each equation fitted is structured and what parameters were selected for fitting the relationships.

2.4.1. Equation type 1: Assuming laminar flow in the karst (Darcian flow or Hagen-Poiseuille equation)

In the case of laminar flow, if we approximate the aquifer as a porous medium, the discharge rates follow the Darcy law:

$$Qr = K*\frac{dH}{dL}*A \tag{1}$$

where K is the hydraulic conductivity of the aquifer at large scale (m.d^{-1}), dH/dL is the hydraulic gradient (where H and L are respectively the hydraulic head and the distance between the borehole where the groundwater level is measured and Kinvarra spring (m)), A is the area through which the flow occurs (m^2).

Alternatively, if we approximate the karst feeding Kinvarra spring as a conduit with laminar flow the discharge rates we can express the Hagen-Poiseuille equation in a similar form to Eq. (1), where K is:

$$K = \frac{{r_{hydr}}^2 * \sigma_0 g}{2\mu} \tag{2}$$

where R_{hydr} is the hydraulic radius of the conduit (m, area divided by wetted perimeter), σ_0 the density of the fluid (kg m^{-3}), g the gravitational constant (m/s^{-2}(−|-)) and μ the dynamic viscosity of the fluid (kg m^{-1} s^{-1}).

Both equations lead to a linear relationship between flow and groundwater level measured close to the main conduit network if $K*A/$

Table 1
Selected water flow estimates coming to Kinvarra Bay, following a previous analysis made by Savatier and Rocha, (2021). For each fieldwork period, we give the average groundwater levels measured at Killiny Borehole (EPA, 2020), and the daily tidal range (Marine Institute, 2020). Radon mass balances give the total SGD flow, while other estimates give the fresh water flow to the bay. Groundwater levels were updated to correspond to daily averages during the exact dates of the surveys.

Date	Groundwater level (m)	Tidal range (m)	Flow (10^5 m^3 d^{-1})	Method	Approximation	Data used	Reference
13–14/07/2018	2.2	5.0	–	Salt balance	Tidal prism B/C Luketina, (1998), with b = 0	24 h sampling at the outlet (Eulerian)	Savatier and Rocha (2020)
22–23/10/2018	3.7	3.9	8.5 ± 1.5				
25–26/01/2019	7.1	4.5	18.6 ± 3.2				
07–08/04/2019	8.8	4.3	18.3 ± 3.2				
13/07/2018	2.1	4.9	1.3		Tidal prism C, Luketina, (1998) with b = 0.86	Transects	Savatier and Rocha (2020)
21/10/2018	3.8	3.2	9.9				
28/01/2019	7.0	2.9	24.2				
06/04/2019	9.2	4.3	15.5				
13/07/2018	2.1	4.9	3.5		Tidal prism with eq. (2) in Cave and Henry, (2011), considering some return of water during floodtide		Savatier and Rocha (2020)
21/10/2018	3.8	3.2	7.8				
28/01/2019	7.0	2.9	13.8				
06/04/2019	9.2	4.3	20.7				
13–14/07/2018	2.2	5.0	4.8			24 h sampling at the outlet	Guerra et al. (in press, as cited in Savatier and Rocha (2020)
22–23/10/2018	3.7	3.9	8.5				
25–26/01/2019	7.1	4.5	14				
07–08/04/2019	8.8	4.3	21				
31/08–01/09/2019	6.5	5.7	12				
Nov-06	6.6	–	12.1			Continuous long-term EC measurements on several locations	Cave and Henry (2011)
Dec-06	10.3	–	19.9				
Jan-07	10.9	–	26.8				
Feb-07	9.3	–	14.7				
03–04/08/2012	4.4	5.5	7.7		Ignore mixing of saline prism, estimates KE + KW only	Transects + continuous measurements	McCormack et al. (2014)
14–15/07/2010	2.4	5.1	2.3 ± 0.5		Steady state, outflow at the outlet is well mixed	Transect + 24 h sampling at the outlet	Rocha et al., (2015)
22–23/06/2011	2.8	2.6	0.8 ± 0.2				
05–07/09/2011	2.5	2.5	0.5 ± 0.2				
23–24/07/2013	1.6	5.6	0.2 ± 0.2				
14–15/07/2010	2.4	5.1	3 ± 1.2	Radon mass balance	Not corrected for spatially variable water ageing	Transect + 24 h sampling at the outlet	Rocha, et al. (2015)
22–23/06/2011	2.8	2.6	0.5 ± 0.2				
05–07/09/2011	2.5	2.5	0.3 ± 0.2				
23–24/07/2013	1.6	5.6	0.2 ± 0.1				
13/07/2018	2.1	4.9	5.2		Corrected for water ageing using Ra relative ages	Transect	Savatier and Rocha, (2020)
21/10/2018	3.8	3.2	9.2				
28/01/2019	7.0	2.9	21				
06/04/2019	9.2	4.3	8.5				
13–14/07/2018	2.2	5.0	5	Daily water balance	Ignore changes of storage with groundwater level + assumed Darcian flow	Groundwater level change, recharge, catchment size.	This study
22–23/10/2018	3.7	3.9	10				
25–26/01/2019	7.1	4.5	18.1				

(continued on next page)

Table 1 (*continued*)

Date	Groundwater level (m)	Tidal range (m)	Flow (10^5 m^3 d^{-1})	Method	Approximation	Data used	Reference
07–08/04/2019	8.8	4.3	23.4				
Annual average	–	–	15.6	Annual water balance	All flow from catchment goes to Kinvarra Bay.	Recharge, catchment size	Schubert, et al. (2015)
min SGD	–	–	4	Not specified	Not specified	Not specified	Drew et al. (2006)
Max SGD	–	–	26				

dL is constant. In Eq. (1), this will be true if fractures linked to the karst network are distributed homogenously vertically (large scale hydraulic conductivity and A remains constant with groundwater level changes). This approach is expected to be a good approximation if groundwater level is measured in areas of the phreatic karst that are connected to the main karst network feeding the karst spring under study, with no impermeable layers of sediment separating the measurement point from the main karst network feeding the karst spring. In our case, this assumption is likely to be valid at large scale, and K is constant with groundwater level if we approximate the aquifer as a porous medium homogenous at large scale. In Eq. (2), K is a constant if the main section of the conduit is always fully submerged (e.g. if springs in Kinvarra bay are fed by a karst network below the minimum groundwater level). If we assume this is the case, we can thus fit in both Eq. (1) using the same regression analysis by modification of the constant KA/dL.

2.4.2. *Equation type 2: The Darcy–Weisbach Colebrook-White equations*

By combining the Darcy–Weisbach equation and the empirical Colebrook-White equation for the friction factor (as shown in Appendix 1) we can find the turbulent flow rate from a tortuous conduit of wetted cross sectional area A and wetted perimeter P as a function of the water height change in the network by:

$$Q = -\sqrt{\frac{16gA^3\Delta H}{\tau\,\Delta LP}}\log_{10}\left(\frac{\varepsilon}{3.7D}+\frac{2.51\nu}{\sqrt{\frac{128gA^3\Delta H}{\tau\,\Delta LP^3}}}\right) \tag{3}$$

where ΔH and ΔL are the head difference and the distance between two locations connected by the conduit (m); A the wetted cross-sectional area of the conduit; P the wetted perimeter of the conduit; g is the acceleration of gravity (m/s^{-2}(−|-)); ν is the kinematic viscosity of the fluid flowing in the conduit (m^2/s), τ is the tortuosity of the conduit (unitless, length of curve per straight distance between two points), ε is the mean roughness height of the conduit microtopography.

We approximate the karst conduit network connecting the Killiny borehole (where the groundwater level is measured) and Kinvarra springs, as a single conduit of a section that is approximately rectangular, variably filled with water, where a turbulent flow towards Kinvarra springs occurs. This type of shape is considered to be a fair approximation for a conduit that developed by preferential dissolution along a fault or other planar discontinuity in the aquifer. Using such assumption, Eq. (3) becomes:

$$Q = \sqrt{\frac{16gy^3b^3\Delta H}{\tau\,\Delta L(y+b)}}\log_{10}\left(\frac{\varepsilon(y+b)}{3.7(2yb)}+\frac{2.51\nu}{\sqrt{\frac{16gy^3b^3\Delta H}{\tau\,\Delta L(y+b)^3}}}\right) \tag{4}$$

where b is the base length of the conduit cross-section, y the average height filled by water in the conduit. y is calculated from the groundwater level at Killiny Borehole (ΔH) minus the water table height at which some flows can occur in the conduit between Killiny Borehole and Kinvarra springs (H_{low}). When the groundwater level is lower than H_{low}, no conduit flows occur to Kinvarra bay. Similarly, the conduit is assumed to stop vertically at a height H_{top}, and when groundwater level reaches levels above it, no additional conduit flow can occur and $y = H_{top}$.

Using Eq. (4) and the observed flow – groundwater level relationships we can thus find b, τ, ε and H_{top} and H_{low} corresponding to the observed flow-discharge relationship. The straight distance between the borehole and Kinvarra spring is $\Delta L \approx 5.2$ km. Similarly, ΔH is the difference of altitude between Kinvarra spring and the groundwater level in Killiny Borehole from the EPA (2020) dataset, and ν the average kinematic viscosity of water. We take $H_{low} = 0$ as no freshwater flow is likely to occur when groundwater level inland is at sea level, and the smallest flows estimated ($Q = 0.2 \times 10^{5}$ m^3/d) were observed in Kinvarra spring for the lowest groundwater level recorded at 1.5 m (Savatier and Rocha, 2021). Tortuosity was taken as $\tau = 1.27$ the median of 35 cave networks previously studied by Collon et al., (2017). Thus b, ε and $Htop$ were used to fit the equation during our regression analysis.

2.4.3. *Equation type 3: Karst network with fractal properties*

From Maramathas and Boudouvis, (2010) the daily average flow occurring at mean sea-level from a spring fed by an aquifer with fractal properties is:

$$Q = a\sqrt{2g(Hs)} \tag{5}$$

where g is the gravitational acceleration constant; Hs is the groundwater table height above the level of the main outlet of the fractal aquifer (here Kinvarra spring); a is a constant specific of the aquifer fractal properties and water volume in the aquifer (Maramathas and Boudouvis, 2010);

In our case, the groundwater level in Kinvarra spring is measured relative to mean sea level, and the average altitude of the point where SGD reach Kinvarra bay is not known. Moreover, the average daily flow derived from tracers is close to zero when the groundwater level inland is above sea level. We thus introduce a correcting factor b to account for this difference. Eq. (5) becomes:

$$Q = a\sqrt{2g(H-b)} \tag{6}$$

where H is the groundwater table height above the level of the main outlet of the fractal aquifer (here Kinvarra spring), and b a correcting factor representing the difference between the effective altitude of discharge to Kinvarra Bay (potentially also affected by head losses) and sea level. This was added to account for the fact that daily averaged flow was close to zero when groundwater was higher than zero (and improved the fit). This parameter b different from zero can be considered as a difference between the "theoretical" level of the spring and the "effective" level of the spring, at which in average most of the discharge occurs. Alternatively, it might represent an approximately constant head loss by friction between the fractal aquifer and the spring discharge point, which may occur for instance if there are restriction impeding the flow (reduction of size of conduit before the spring). The relationship (6) thus was fitted using the a and b parameters.

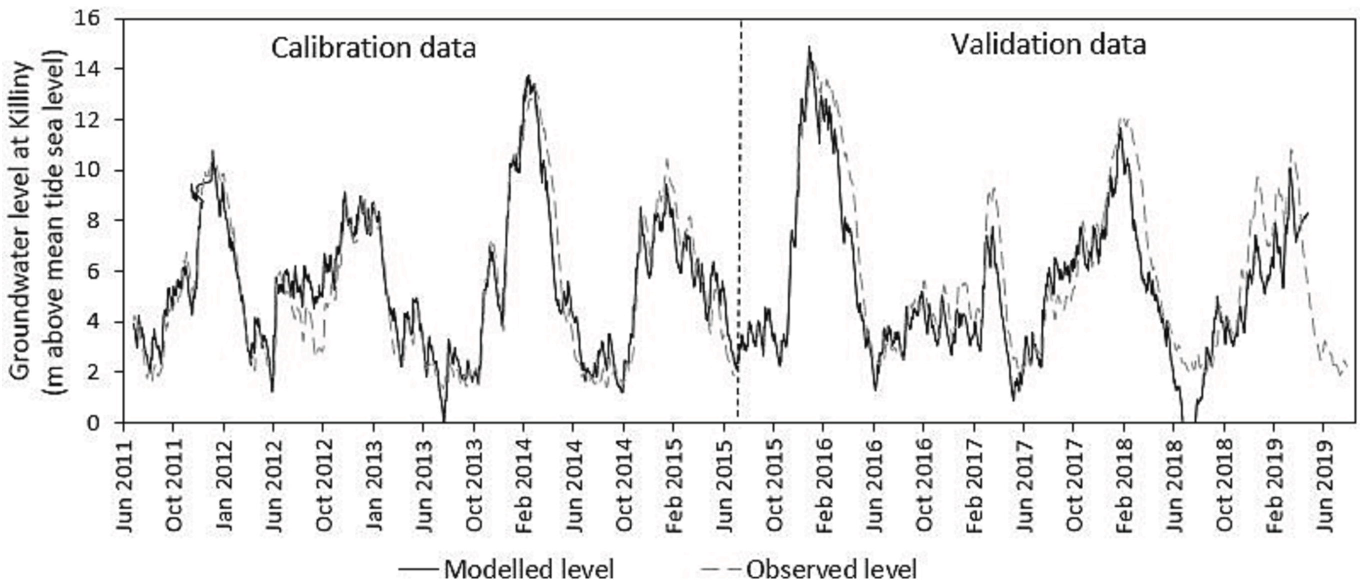

Fig. 2. Validation of a daily water balance approach using groundwater level measured by the EPA at the Killiny borehole (EPA, 2020).

2.5. Daily water balance

We can express a daily water balance for the aquifer as:

$$\Delta S = P - E - Qr - M \tag{7}$$

where ΔS is the change of storage in the aquifer for a given day, P is the precipitation and E is evapotranspiration in the catchment, Qr is the flow of Kinvarra spring in one day and M is the additional abstractions from pumping each day in the area (all terms in $m^3.d^{-1}$). The main groundwater abstraction in this area feeds the town of Kinvarra with drinking water supply with an average abstraction rate of 1440 m^3/d. Private boreholes are also present in the catchment and may add to this abstraction value. The total M value is thus unknown to date. However, most previous works on Kinvarra spring flows suggest flow rates larger than $5x10^5$ m^3d^{-1}, which implies that abstraction will play a minor role in the water balance variability unless in particularly dry periods. According to some estimates abstraction might be more significant during severe droughts periods (with the lowest estimate of discharge from Kinvarra spring being $2x10^4$ m^3/d, Table 1). However, even during these periods a good part of the water abstracted in this area is then discharged back to groundwater via percolation areas in houses. With current water usage we do not expect abstraction to make a large difference in the annual water balance. For this annual intercomparison, and in the absence of data on the variability of M, we thus neglect M, the effect of which is negligible during low-medium to medium to high flow periods (flows in Table 1 are generally far above 10^5 m^3/d).

The relationship between groundwater level and the storage in the aquifer can be given using the volumetric specific storage:

$$\Delta S = Va^*Ss^*\Delta H \tag{8}$$

where Ss is the volumetric specific storage (m^{-1}), Va the bulk volume of the portion of the aquifer from which the volume is released (m^3), ΔH the hydraulic head change (m).

Assuming Darcian flow (equation type 1), and using Eq. (5), the water mass balance (Eq. (7) becomes:

$$Va^*Ss^*\Delta H = \frac{KA}{dL}{}^*dH + P - E \tag{9}$$

This can be rearranged to express the groundwater height at day n + 1 as a function of the water table height measured the previous day:

$$H_{n+1} = \frac{\left(\left(\frac{KA}{dl} - VaSs\right)^*H_n + P - E\right)}{Va^*Ss} \tag{10}$$

If we make $X = \frac{KA}{dL} and Y = VaSs$, this becomes:

$$H_{n+1} = \frac{((X - Y)^*H_n + P - E)}{Y} \tag{11}$$

An eight-year long (June 2011 to Nov. 2019) groundwater and meteorological dataset was used to find the values of X and Y and validate the model. For this purpose, we divided the data set into two parts, the first for calibration (to find the X and Y parameters using least squares fitting) and the second part was used for validation of the data. We then used the value of X to independently evaluate the model predictions of fresh SGD for any groundwater level from Eq. (1) against prior tracer and hydrogeological modelling estimates. Rainfall and evaporation data to close the daily water balance were taken from the Athenry meteorological station, 20 km from Kinvarra Bay (Met Eireann, 2020).

3. Results

3.1. Daily water balance

The daily water balance reproduced the general seasonal groundwater level variability at Killiny Borehole (Fig. 2). The coefficient of determination between modelled and observed groundwater level for the validation period was 0.86, suggesting an acceptable fit. The modelled groundwater levels decreased faster than the observed levels at the end of periods of high groundwater level, leading to a maximum difference of 2.5 m, potentially due to the changes of storage associated with flooding of turlough and the effect of superficial drainage, not considered in this simplified model.

This model resulted in: $X = 2.49{*}10^5$ $m^2.d^{-1}$ and $Y = 1.07{*}10^7$ m^2 (parameters in Eq. (10), 11). This simplified estimate provides us with a base of comparison, which will be used to compare with the tracer-based estimates and results from the more complex hydrogeological models.

3.2. Comparison between daily average fresh SGD estimates

All previous studies' fresh SGD estimates from salt mass balances and tidal prism methods (Cave and Henry, 2011; McCormack et al., 2016;

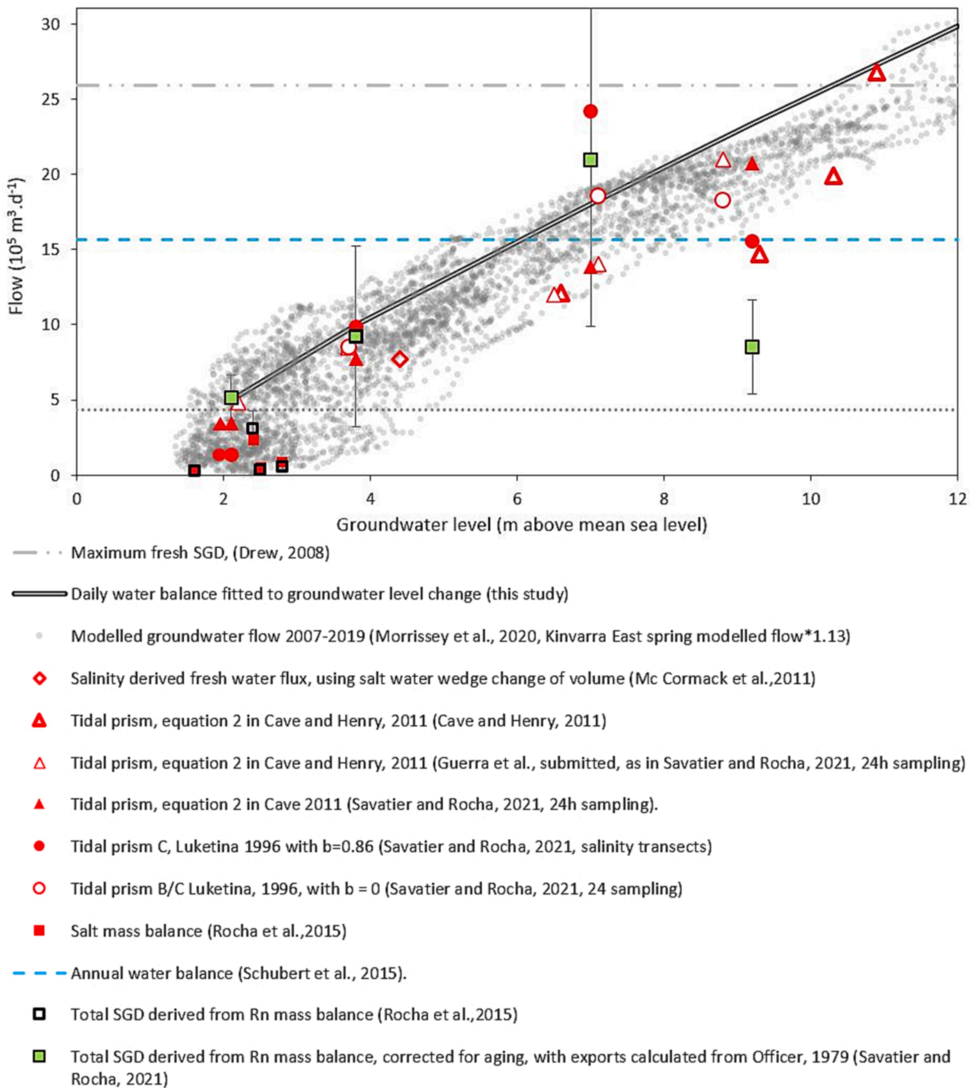

Fig. 3. Comparison between daily SGD estimates in Kinvarra bay as a function of groundwater level at Killiny Borehole. The modelled flows from Morrissey et al., (2020) are multiplied by 1.13 to account for the additional recharge occurring from the Kinvarra East spring catchment not included in the main hydrogeological model.

Rocha et al., 2015; Savatier and Rocha, 2021) and from hydrogeological modelling (Morrissey et al., 2020) as described in Section 2.2, are shown in Fig. 3 and Table 1. There is a highly significant monotonic positive correlation between groundwater level and flow rates (Spearman correlation: 0.84, with p value: 7.1×10^{-10}). For example, fresh SGD estimates derived from the tidal prism method range from 0.2×10^5 m^3/d at low groundwater levels (1.6 m) to 26.8×10^5 m^3/d at high groundwater levels (10.9 m, Table 1). Estimates of total SGD (fresh + saline SGD) follow similar trends, going from 0.2×10^5 m^3/d at low groundwater levels (1.6 m, Table 1) to 21×10^5 m^3/d at medium to high groundwater levels (7 m, Table 1). However, one exception to this trend is the estimate for groundwater level 9.5 m which is only at 8.5×10^5 m^3/d (Savatier and Rocha, 2021) (Fig. 3, Table 1). Most of the SGD estimates from tracers and hydrogeological models are within the range put forward by Drew (2008) and the relationship between groundwater level and flow is consistent with the estimates from water budgets developed in Schubert et al. (2015a).

Conversely, the Spearman correlation coefficient between tidal range and the daily averaged fresh and total SGD for the range observed so far is −0.16 with a p-value of 0.37 (2.5 to 5.6 m, Table 1 and Fig. 3). Thus, there is no significant monotonic function between tidal range and SGD (as also visible graphically in Fig. 4). This suggests that in this case, the groundwater level variation above sea level explains a greater proportion of the variability of SGD than tidal variability alone.

If we focus on the 2018–2019 period for which the most recent flow estimates were made (Morrissey et al., 2020; Savatier and Rocha, 2021), the estimates of SGD from salt and radon budgets are generally similar to or larger than flows modelled by Morrissey et al. (2020) for the 2018–2019 period, except during April 2019, where they are similar or lower (Fig. 5). Similarly, radon-based estimates are always within the range of the salt-derived estimates except for April 2019, where they are significantly lower than estimates produced by the Morrissey et al. (2020) model (Fig. 5).

The Morrissey et al. (2020) model predicts lower SGD values for groundwater level 2 m than those suggested by tracer-based estimates for this period (July 2024, Fig. 5). This difference may be explained from the large uncertainty of tracer-based estimates and/or if other more minor springs (compared to Kinvarra East and West springs) are active during low groundwater level periods providing more diffuse flows to the bay.

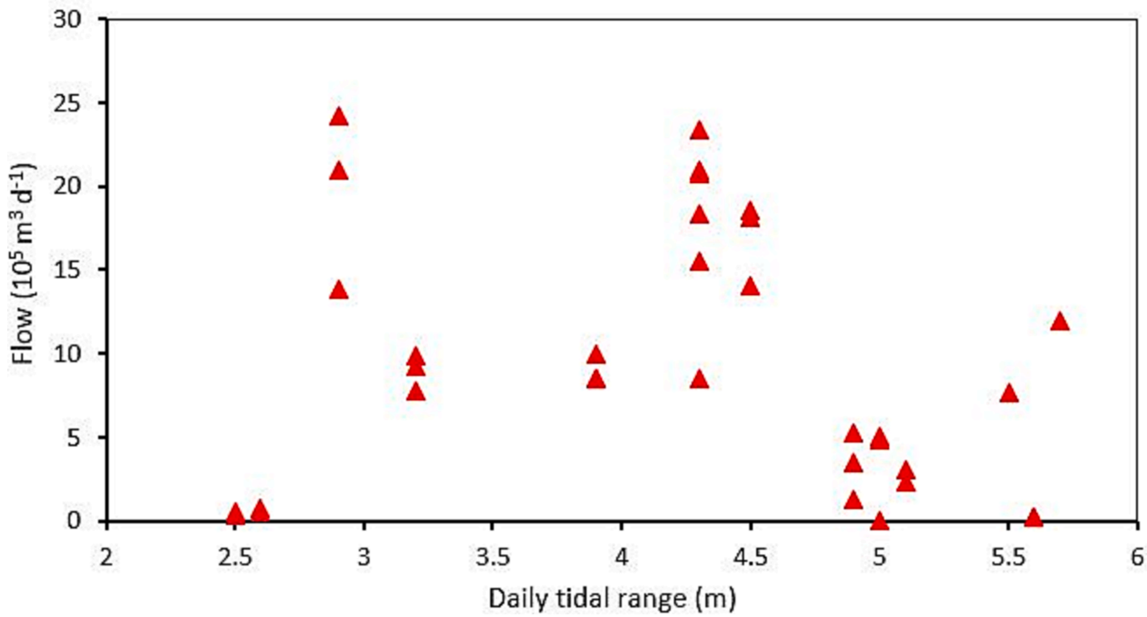

Fig. 4. Daily averaged fresh SGD flow and daily tidal range are not correlated.

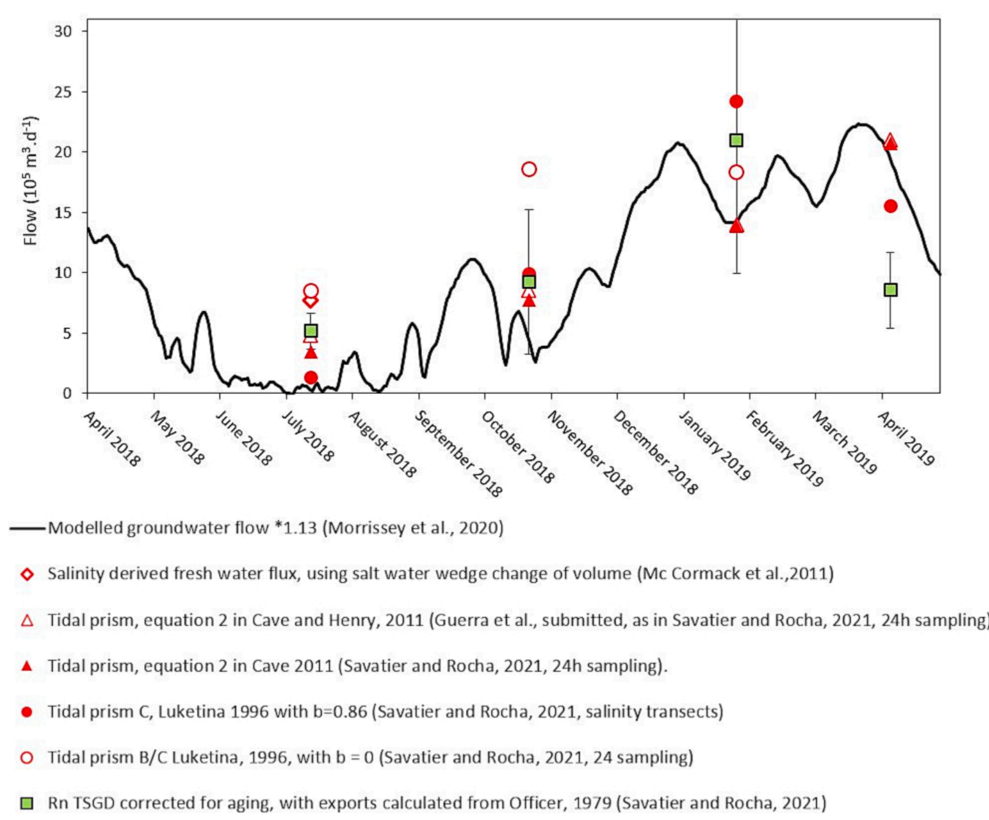

Fig. 5. Comparison between tracer-based estimates and daily averaged modelled flow rates from the hydrogeological model during the 2018–2019 period. The modelled flows from Morrissey et al., (2020) are multiplied by 1.13 to account for the additional recharge from the Kinvarra East spring catchment, not included in the main hydrogeological model.

3.3. Relationship between fresh SGD and groundwater level

3.3.1. Comparison with discharge estimates from tracers

The three alternative relationships between groundwater level and SGD (Darcian flow, Fig. 6 a; Darcy–Weisbach Colebrook-White equations Fig. 6 b; Non Darcian flow in a fractal aquifer, Fig. 6 c) fit the data well for medium groundwater levels, with most points within the 95th % prediction interval. Considering the lateral spread of the data and the large uncertainty of the flow estimates, these results raise further confidence on the internal consistency of the methods previously used to estimate flow in Kinvarra Bay. The second and third relationship (Fig. 6 b, c) give a better estimate of the range of freshwater flows for

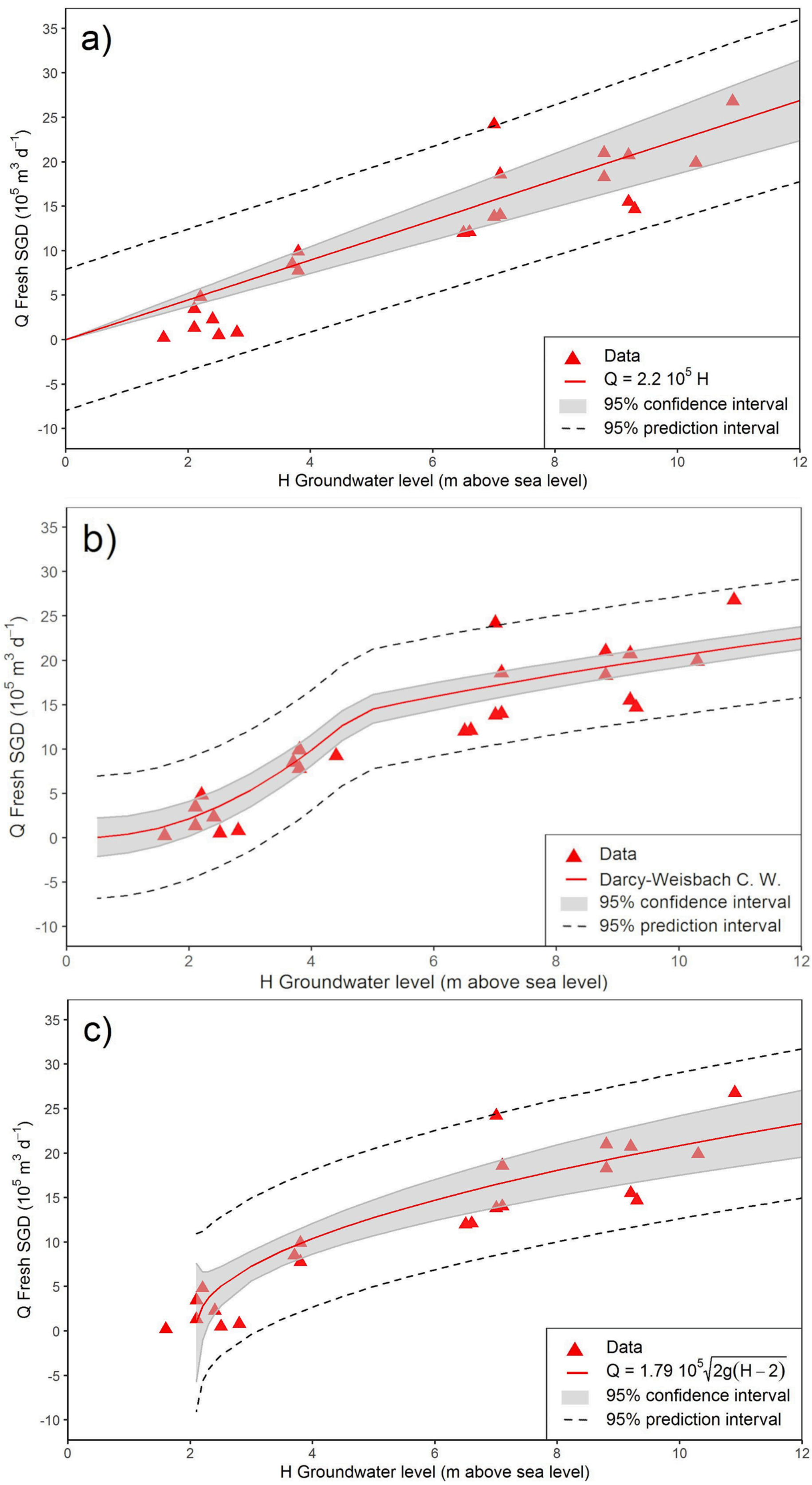

Fig. 6. Relationship between fresh SGD estimates based on salinity from Table 1 and groundwater level on the day of the survey, (a) assuming Darcian flow; (b) assuming dominant conduit flow with turbulent flow (Darcy–Weisbach Coolebrook-White equations with Htop = 4.8, b = 6.4, ε = 2.1) and a main karst network between 0 and 7 m above mean sea level; or (c) assuming an aquifer with fractal properties and an average flow occurring at a level different than mean sea level. For the fit using the Darcy–Weisbach Coolebrook-White equations a simplified method is used for the estimation of the 95th % confidence and prediction interval (cf. Annex 2).

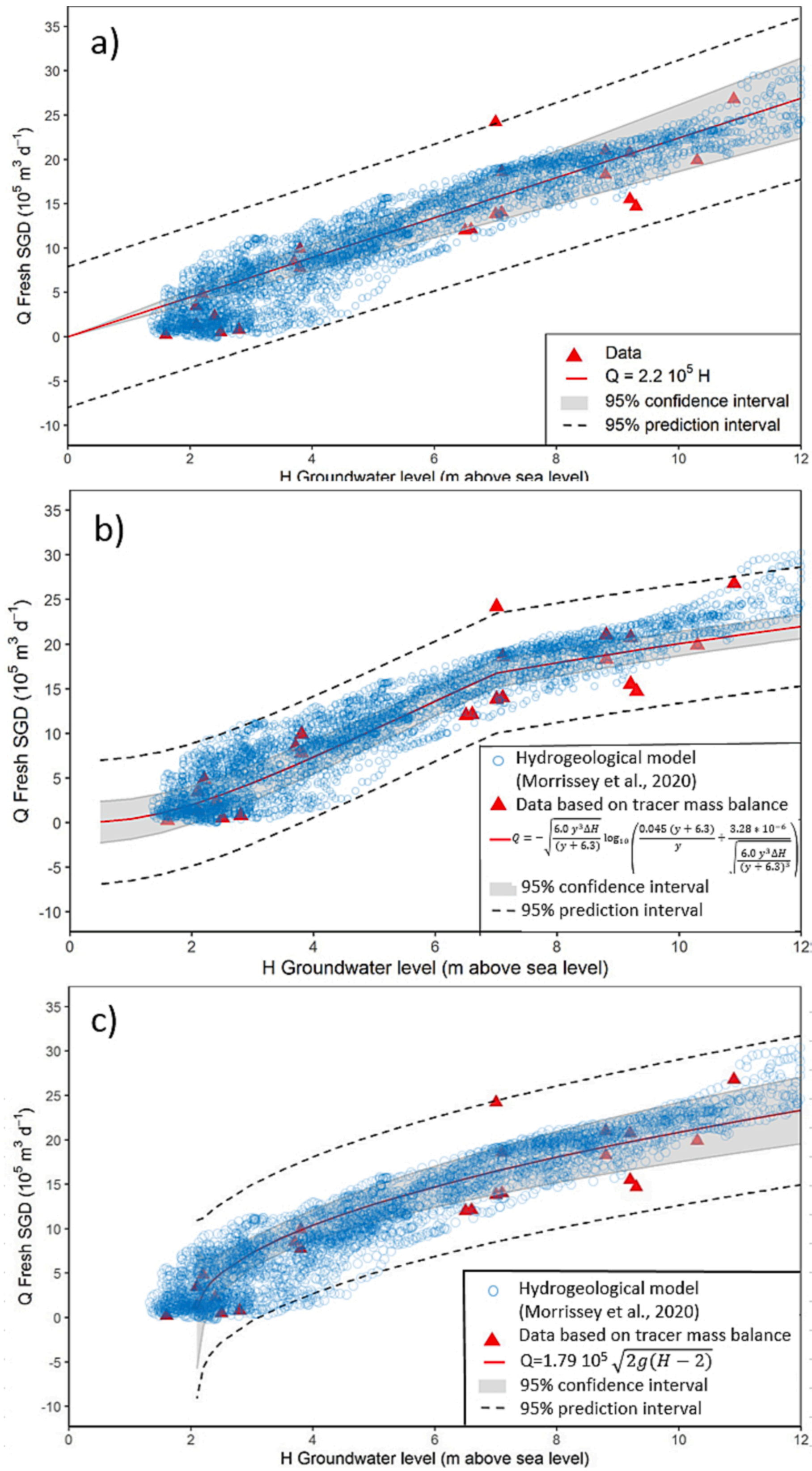

Fig. 7. Comparison of hydrogeological model results (Morrissey et al., 2020) for the 2007–2019 period with tracer derived flow data and relationship derived from tracer-based fresh SGD estimates: (a) fitted with the Darcy equation, (b) fitted with the Darcy–Weisbach Coolebrook-White equations assuming turbulent conduit flow with Htop = 4.8, b = 6.4, ε = 2.1, (c) fitted with the Toricelli formula adapted for fractal networks, assuming a karst with fractal properties. Modelled flow rates from the hydrogeological model (Morrissey et al., 2020) are shown with blue dots, with darker colour with increasing density of points. Flow rates from this model were multiplied by 1.13 to convert Kinvarra East flow rate into total flow rates. The 95th % confidence and prediction interval for discharge shown in figure 8a are likely to be underestimates of uncertainty as a linearization approximation had to be used to estimate them (see appendix 2 for the details on parameters uncertainty). (For interpretation of the references to colour in this figure legend, the reader is referred to the web version of this article.)

Table 2
Fitted model parameters and their estimated uncertainties (expressed as 95th % confidence interval).

Model type	Method to fit the model and calculate parameter uncertainty	Method to calculate uncertainty of discharge	Fitted model parameter		
			Name	Fitted value ± 95th % confidence interval	95th % confidence interval (% of fitted value)
Darcy model	Least square minimisation with Gauss-Newton algorithm (using R non-linear solver)	Higher order taylor expansion and montecarlos simulation propagate R package (Spiess, 2018)	K A/dl	2.2 ± 0.4	17 %
Darcy–Weisbach Colebrook-White equations			Conduit top height y	4.8 ± 3	62 %
			Conduit width b	6.4 ± 35.2	550 %
			Conduit roughness ε	2.1 ± 33.5	1300 %
Fractal model			a	1.8 ± 0.3	17 %
			b	2 ± 0.4	22 %

groundwater levels below 3 m and groundwater levels above 9 m, with more points closer to the 95th % confidence interval.

3.3.2. Comparison with discharge estimates from hydrogeological model

While model predictions from the hydrogeological model are linear for groundwater levels above 4–5 m, at groundwater levels below 3 m we observe an increase of slope as we get closer to 1.5–2 m groundwater level. This change of slope corresponds well to the expected trend for a fractal aquifer we derived independently from our third relationship (Fig. 6c), and for the expected trend for a single conduit with turbulent flow feeding Kinvarra spring (Fig. 6b) but less so to the first relationship based on purely Darcian flow (Fig. 6a). The estimates of SGD from the hydrogeological model results (Morrissey et al., 2020) are mostly within the 95th % predicted interval for the three relationships (Fig. 7). Moreover, most points predicted by the hydrogeological model are close to or within the 95th % confidence interval of the second and third relationships for groundwater less than 9.5 m (Fig. 7). Above 9.5 m, the hydrogeological model can predict larger flow values than suggested by the 95th % confidence interval, which suggest that this model will be less accurate during severe flooding conditions. However, only a few points (<0.5 % of daily values) are higher than the 95th % prediction interval.

This suggests that a simple approach approximating the behaviour of a karst aquifer from its fractal properties can lead to first-order relationships consistent with the flow variability with groundwater level suggested by hydrogeological models approximating the karst as a series of interconnected conduits (McCormack et al., 2014; Morrissey et al., 2020). The Darcy–Weisbach Colebrook-White equations may also perform well for these conditions but requires more information on the nature of the karst network to fit the flow-groundwater level relationship (shape, size, altitude, tortuosity and roughness of conduit). The uncertainty of the fitted parameters is also much larger for the Darcy–Weisbach Colebrook-White equations than for the fractal equation when estimating using Monte Carlo analysis and Taylor expansion series (see Appendix 2: Fitted parameters of the three models and their uncertainty estimation). The Darcy equation, on the other hand provided a fair estimate of fresh SGD when groundwater level was at intermediate levels, but overestimated SGD when groundwater level was at low or high levels (droughts or high recharge conditions).

4. Discussion

Our cross-analysis of multiple methods to assess SGD in coastal sites showed that: (1) daily averaged estimates coincide with groundwater table variability after a systematic review and validation of the methods' assumptions for the bay under study (e.g. Savatier and Rocha, 2020); and (2) a simplified relationship between fresh SGD and groundwater table height next to a conduit near the coast can be derived for management purposes. Three types of approximations were tested to derive relationships between near-conduit groundwater level and flow: (a) a linear relationship between groundwater level and flow, assuming Darcian flow in the karst, (b) a non-linear approximation using the Darcy–Weisbach Colebrook-White equations, approximating the karst between Killiny Borehole and Kinvarra springs as a single phreatic conduit carrying most of the flow to the bay, (c) a fractal approximation, approximating the karst as a network with fractal properties. Methods (a) (b) and (c) performed equally well for medium groundwater levels (between 4 and 9 m at Kinvarra), but methods (b) or (c) corresponded better to the flows predicted by a complex hydrogeological karst network model of the catchment for low and high groundwater level when a non-linear change was observed between groundwater level and fresh SGD (Fig. 6). We also remind the reader that for method (b) a simplification is used in this work to estimate the confidence interval of parameter uncertainty with three fitted parameters (see annex 2 for more detail and justification as to why a simplified method was preferred). Using a three parameter expression, the higher order Taylor expansion and Monte Carlo analysis leads to large confidence and predictive interval of parameter and flow uncertainty for method (*b*). This uncertainty is significantly lower if only two parameters are unknown (see annex 2 for more detail).

When groundwater levels are less than 11 m, the flows given by the Morrissey et al., (2020) hydrogeological model were within the 95th % prediction interval and close to or within the 95th % confidence interval of the fits approximating the aquifer as a fractal network or as a single dominant conduit with turbulent flow (Darcy–Weisbach / Colebrook-White equations). This suggests that daily SGD from this system can be well predicted by the fractal approach, as well as using the hydrogeological model for this range of flow. Above 11 m, the flow rate predictions of the Morrissey et al., (2020) model significantly deviate from the fractal or the Darcy–Weisbach /Colebrook White approximation, with some values above the 95th % prediction interval of these relationships. It is likely that above such high groundwater levels, the effect of water storage in turloughs and other groundwater-surface interactions (river complete infiltration in the karst network, transient storage of groundwater above ground in turlough or their associated floodplains), considered with more realism in the Morrissey et al., (2020) model, explain this difference. However, due to the absence of tracer-based discharge estimates by other methods at groundwater levels above 11 m (Fig. 3 and Table 1) it is not possible to provide any confidence as to which range of groundwater flow is the most likely to discharge into the bay during such periods. As previously highlighted (see Fig. 1), the nearby Aughinish Bay also receives groundwater inputs during winter and periods of significant rainfall (Smith and Cave, 2012), when the groundwater level is most likely to be the highest. Although this conduit does not appear to feed Aughinish bay significantly outside of the flood periods (Smith and Cave, 2012), we can expect some groundwater flows to be redirected to Aughinish Bay when groundwater levels are high, thus reducing the flow rates expected for these groundwater levels. Thus, additional tracer-based estimates of SGD could be made at groundwater levels above 11 m (at Killiny borehole) to

Table 3
Effect of the fitting method on the parameter values and their uncertainty for the Darcy–Weisbach Colebrook-White equations.

Method to fit the model and calculate parameter uncertainty	Method to calculate uncertainty of values	Model parameter		
		Name	Fitted value ± 95th % confidence interval	95th % confidence interval (% of fitted value)
Generalized Reduced Gradient Non-linear solver (excel) (solution if start value Htop = 5, b = 3, ε = 0.05)	Regression analysis assuming that uncertainty distribution is similar to the one of a linear regression.	Conduit top height y	4.4	Unknown
		Conduit width b	13.2	Unknown
		Conduit roughness ε	9.0	Unknown
Generalized Reduced Gradient Non-linear solver (excel) (solution if start value Htop = 7, b = 2, ε = 0.01)	Regression analysis assuming that uncertainty distribution is similar to the one of a linear regression.	Conduit top height y	7	Unknown
		Conduit width b	1.8	Unknown
		Conduit roughness ε	0.01	Unknown
Evolutionary Non-linear solver (excel) (solution if start value Htop = 5, b = 3, ε = 0.05)	Regression analysis assuming that uncertainty distribution is similar to the one of a linear regression.	Conduit top height y	4.4	Unknown
		Conduit width b	13.1	Unknown
		Conduit roughness ε	8.9	Unknown
Evolutionary Non-linear solver (excel) (solution if start value Htop = 7, b = 2, ε = 0.01)	Regression analysis assuming that uncertainty distribution is similar to the one of a linear regression.	Conduit top height y	4.4	Unknown
		Conduit width b	13	Unknown
		Conduit roughness ε	8.9	Unknown
Gauss-Newton algorithm (using R non-linear solver)	Higher order taylor expansion and montecarlos simulation propagate R package (Spiess, 2018) with b constant = 6.4	Conduit top height y	4.8 ± 1.4	29 %
		Conduit roughness ε	2.2 ± 2	93 %
	Higher order taylor expansion and montecarlos simulation propagate R package (Spiess, 2018) with e constant = 2.1	Conduit top height y	4.8 ± 1.5	32 %
		Conduit width b	6.4 ± 2.1	33 %

(a) determine if this effect is significant for the flow to Kinvarra bay and to (b) improve the simple relationships based on fractal approximation or the Darcy–Weisbach / Colebrook-White approximations for these high discharge conditions. Nevertheless, groundwater levels measured at Killiney Borehole were below 11 m more than 93 % of the days between 2007 and 2019. Thus, until new flow estimates measurements are available for these high discharge conditions, we expect the current fits to provide an acceptable assessment of the annual variability of fresh SGD each year for most days in this system.

Without continuous measurement of SGD tracers in the bay, we cannot, however, be sure that the relationship between groundwater level and daily averaged freshwater discharge will stand for any day. Exceptions may occur as a result of density-driven SGD and the seaward movement of the fresh/seawater interface (Kohout, 1965). Moreover, for the use of equation of this type in other karst systems, it is important to highlight that the type of head discharge relationship may be distinct between phreatic conduits and superficial conduits: epikarst conduits may be more strongly non-linear (e.g. as highlighted by Jeannin, 2001). The measurement point for groundwater level used in this study is a borehole connected to a deep phreatic conduit. The relationship between groundwater discharge and head observed here is similar to the one observed by Jeannin, (2001) for a deep phreatic conduit in the Holloch cave, which suggests that the method used here may be appropriate for other karsts with phreatic conduits. This suggests that these relationships, once fitted with appropriate flow and groundwater level data for a specific site, are likely to lead to a reasonable forecast of the general annual variability of water flow from karst aquifers to coastal areas. In particular they are likely to apply in sites where the head variability due to net recharge is larger than the variability of sea level, and where groundwater level can be measured in a point connected to a phreatic conduit (in such sites, daily averaged fresh SGD becomes mainly dependent on groundwater level).

It should be kept in mind that discharge of coastal springs in karst may also contain a large fraction of saline water, depending on the connectivity of the karst conduit with the sea (Fleury et al. 2007). Where these saline fluxes occur in diffuse karst network and/or coastal sediments, their magnitude and effect on solute fluxes may be challenging to quantify, as multiple solute sources may be present with distinct properties. In Kinvarra Bay, an increase of radium activities was observed during summer, low groundwater level periods. This was attributed to fluxes of saline SGD of between 0.5×10^5 m^3/d to 80×10^5 m^3/d depending on the dominant water pathway creating the Ra release, potentially bringing new nutrients such as phosphorus (Savatier, 2021). Such inputs can amplify phytoplankton growth in coastal areas and require characterisation in addition to the fresh SGD inputs. Similar first-order relationships might be derived for saline SGD under certain conditions, to help decision making in SGD sites (Savatier, 2021). However, more estimates of both recirculated and fresh SGD are required to develop such relationship for recirculated SGD.

Simple relationships describing the temporal variability of SGD are valuable for coastal managers and decision-makers when long term predictions have to be made on potential trends, before a more detailed assessment can be made. For example, to develop optimal management of groundwater resources to preserve coastal ecosystem value for human activities (e.g. Pongkijvorasin et al., 2010).

The lowest SGD values are found during periods when groundwater levels ranged between 1.7 and 2.2 m above mean tide level (Fig. 3). Three hypotheses may explain these low, close to zero flows when the groundwater head is still above sea level: (1) the main spring altitude is above mean sea level at an altitude between 1.7 and 2.2 m; (2) there is a head loss of 1.7–2.2 m within the karst conduit between the measurement point and the spring, preventing flow when groundwater level is too low; (3) there is both a head loss and a spring altitude above mean sea level.

The altitude of Kinvarra springs, as estimated from Infomar data, is between 1.9 and 3.9 m above the lowest astronomical tide level. This is equivalent to −1.4 and + 0.5 m above mean sea level, thus much lower than the observed transition point (Fig. 3). Unless other springs at higher altitude are present contributing to the head loss, it is thus likely that a non-linear head loss is present within the karst system. This further suggests that equation type 2 and 3, which account for head loss due to turbulent flow, are more appropriate than an equation assuming a Darcian, laminar only flow.

Finally, one total SGD estimate derived from radon mass balance was lower than suggested by the groundwater level discharge-flow relationship derived from other surveys (April 2019 survey, Table 1 and Fig. 3). Such low estimates were previously attributed to the variable water exchange between Kinvarra Bay and Galway Bay and its effect on non-conservative tracers (Savatier and Rocha, 2021).

5. Conclusion

An intercomparison study of a range of catchment-based and tracer-based methods to assess submarine groundwater discharge from a lowland karst catchment to an enclosed bay has been presented. It is generally not feasible to measure directly the total discharge from submarine springs entering a bay as flows can occur through multiple diffuse karst networks, and tracer based and catchment-based methods are thus used to close this knowledge gap. They enable the total discharge coming into a bay to be assessed when they are based on assumptions appropriate for the study site, but it may be difficult in practice to verify the assumptions taken. Comparing discharge estimates from multiple methods to cross validate them generally requires the studies to be carried out across the same dates, which can be time and resource demanding. These may also prevent the observation of disparities between method variables with time (for example due to changes of flushing during high groundwater flow periods). On the other hand, hydrogeological models can simulate the total discharge from a groundwater catchment into coastal bays but depend upon being thoroughly calibrated and validated on real data collected in the catchment across the same periods for their simulated flow rates, and extensive knowledge of the catchment limits and of preferential flow pathways. To overcome these obstacles, and facilitate the comparison and cross validation of studies carried out in the last thirty years in Kinvarra bay, we used as a standard reference continuous measurements of groundwater level in direct proximity to a karst conduit feeding the main springs of the bay during the same period. Using this approach, we show that tracer-based estimates and catchment-based estimates all suggest a relationship between groundwater level -measured close to this preferential water flow pathway- and flow, as expected, and that they match fairly well between each other. We use the pooled results to test three types of first-order relationships between groundwater level and fresh SGD in a karst system. Relationships assuming Darcian or laminar flow in the karst fitted the flow-groundwater level dataset well for medium groundwater levels, but overestimate discharge during high and low groundwater level periods. Relationships using the Darcy–Weisbach / Colebrook-White equations or approximating the karstic aquifer as a fractal network performed better for these high and low level conditions, and fitted equally well the data for medium flow conditions. Furthermore, flow predictions from a more complex hydrogeological model calibrated independently by a previous study were within the 95th % prediction interval of these two equations when groundwater levels were less than 11 m. However, at groundwater level above 11 m the hydrogeological model predicts significantly larger flows than expected from the two simple flow-discharge relationships. However, no flow predicted data is available for these conditions above 11 m yet by other methods, and so it is not possible to corroborate or otherwise such predicted flow rates. Nevertheless, we can expect the more complex hydrogeological model to represent the discharge into the bay more confidently across these higher range of groundwater levels, as the complexity of variable storage in turlough and groundwater-surface interactions in the catchment are accounted more accurately. On the other hand, events not accounted for in this hydrogeological model are also possible and could lead to reduced fluxes during high groundwater periods. For example, there is previous evidence that some of the groundwater flow in the conduit feeding Kinvarra springs may be diverted via an overflow to the nearby Aughinish Bay during high groundwater level periods. To conclude, most previous intercomparison studies have not compared SGD fluxes estimates across a full range of groundwater level variability observed during the year. We illustrate that doing so is crucial to understand such coastal systems, in particular when connected to karstic areas, where fresh SGD fluxes can be multiplied by ten or more with rising groundwater level and multiple water pathways can be present. Intercomparison studies accounting for time variability need to be carried out more frequently as they: (1) enable validation of SGD estimates from multiple methods and periods; (2) derive the annual variability of SGD fluxes from which optimum management strategy of coastal bays can be developed; and (3) assess the limits of models used to evaluate SGD fluxes.

CRediT authorship contribution statement

Maxime Savatier: Conceptualization, Methodology, Software, Formal analysis, Investigation, Data curation, Writing – original draft, Writing – review & editing, Visualization. **Patrick Morrissey:** Conceptualization, Methodology, Investigation, Writing – original draft, Writing – review & editing. **Laurence Gill:** Conceptualization, Methodology, Resources, Writing – original draft, Writing – review & editing, Supervision, Funding acquisition. **Carlos Rocha:** Conceptualization, Resources, Writing – original draft, Writing – review & editing, Supervision, Funding acquisition.

Declaration of Competing Interest

The authors declare that they have no known competing financial interests or personal relationships that could have appeared to influence the work reported in this paper.

Data availability

Data will be made available on request.

Acknowledgment

This publication is a result of research supported in part by a research grant from Science Foundation Ireland (SFI) under Grant Number 13/RC/2092 and co-funded under the European Regional Development Fund and industry partners of the Irish Centre for Research in Applied Geosciences (iCRAG). Maxime Savatier was supported through an iCRAG PhD fellowship (ref TP GW3.2PhD5), co-funded by Science Foundation Ireland (SFI) and the European Union.

This work was also carried out as part of the scientific project “GWFlood: Groundwater Flood Monitoring, Modelling and Mapping”, funded by Geological Survey Ireland, and also represents outputs from research funded by the Office of Public Works and the Irish Research Council. The authors would like to thank the Irish Meteorological Service (Met Eireann) for the provision of rainfall data, Galway County Council for the provision of aerial photography and GIS data, and the Office of Public Works for the provision of LIDAR, hydrometric and aerial photography data used for the development of the hydrogeological model of the karst.

Appendix 1:. Demonstration of the combined Darcy–Weisbach and Colebrook-White equations used in part 2.4.2

For turbulent flow rate through a pipe or conduit (Reynolds number > 4000), the head loss by friction is defined empirically by the Colebrook-White equations:

$$\frac{1}{\sqrt{f}} = -2log_{10}\left(\frac{\varepsilon}{3.7D}+\frac{2.51\nu}{DV\sqrt{f}}\right) \tag{a1}$$

Where f is the friction factor (unitless), ε is the mean roughness height of the conduit wall micro-topography (m), D is the hydraulic diameter of the conduit (here four times the wetted cross section divided by the wetted perimeter of the conduit), V is the mean velocity of the flow in the conduit (m/s), ν is the kinematic viscosity of the fluid (m^{-2} s^{-1}).

From the Darcy–Weisbach equation the head loss (ΔH, m) per length (C, m) in a pipe is:

$$\frac{\Delta H}{C} = \frac{fV^2}{2gD} = \frac{fQ^2}{2gDA^2} \tag{a2}$$

So,

$$f = \frac{\Delta H}{C} \cdot \frac{2gD.A^2}{Q^2} \tag{a2 bis}$$

where g is the gravitational acceleration constant (m/s^{-2}(−|-)), A is the cross-section area filled with water in the conduit (m^2), Q is the flow rate crossing the cross section of the conduit (m^3/s). If we consider that the conduit goes between two points following a curve of tortuosity τ, equal to the curve length (C) divided by the straight distance between the two points (ΔL), we can replace C by $\tau\Delta L$ in Eq. (a2) to account for the tortuosity of the conduit and find f as:

$$f = \frac{2gD\Delta H}{\tau \Delta L V^2} = \frac{2gDA^2\Delta H}{\tau \Delta L Q^2} \tag{a3}$$

By inserting Eq. (a3) in Eq. (a1) we can express the combined the Darcy–Weisbach and Colebrook-White equations as:

$$\frac{1}{\sqrt{\frac{2gDA^2\Delta H}{\tau \Delta L Q^2}}} = -2log_{10}\left(\frac{\varepsilon}{3.7D} + \frac{2.51\nu}{D\frac{Q}{A}\sqrt{\frac{2gDA^2\Delta H}{\tau\Delta L Q^2}}}\right)$$

Then: $\frac{Q}{\sqrt{\frac{8gDA^2\Delta H}{\tau\Delta L}}} = -\log_{10}\left(\frac{\varepsilon}{3.7D} + \frac{2.51\nu}{D\sqrt{\frac{2gD\Delta H}{\tau\Delta L}}}\right)$ extracting Q we obtain:

$Q = -\sqrt{\frac{8gDA^2\Delta H}{\tau\Delta L Q^2}}\log_{10}\left(\frac{\varepsilon}{3.7D} + \frac{2.51\nu}{D\sqrt{\frac{2gD\Delta H}{\tau\Delta L}}}\right)$ then:

$$Q = -\sqrt{\frac{8gDA^2\Delta H}{\tau\,\Delta L}}\log_{10}\left(\frac{\varepsilon}{3.7D} + \frac{2.51\nu}{\sqrt{\frac{2gD^3\Delta H}{\tau\,\Delta L}}}\right) \tag{a4}$$

From which we can find for example the equation from Horlacher and Lüdecke, (1992), in Shoemaker et al., (2008) used in MODFLOW CFP for circular conduits, after replacing A with its value for conduits of circular cross-sections ($\pi D^2/4$).

If we include in equation a(4) the definition of the hydraulic diameter ($D = 4A/P$) we thus have the general equation for the combined Darcy–Weisbach Colebrook-White equations:

$$Q = -\sqrt{\frac{32gA^3\Delta H}{\tau\,\Delta LP}}\log_{10}\left(\frac{\varepsilon P}{3.7^*4A} + \frac{2.51\nu}{\sqrt{\frac{128gA^3\Delta H}{\tau\,\Delta LP^3}}}\right) \tag{a5}$$

where P the wetted perimeter of the conduit cross-section.

In the case of a conduit of rectangular section of base b and height filled with water y (thus area $A = b.y$ and wetted perimeter $P = 2(y + b)$) we thus have the equation used in this work for a conduit with rectangular cross section:

$$Q = -\sqrt{\frac{16.gy^3b^3\Delta H}{\tau\Delta L(y+b)}}log_{10}\left(\frac{\varepsilon(y+b)}{3.7(2yb)} + \frac{2.51\nu}{\sqrt{\frac{16gy^3b^3\Delta H}{\tau\Delta L(y+b)^3}}}\right) \tag{a6}$$

Appendix 2:. Fitted parameters of the three models and their uncertainty estimation

Table 2 shows the fitted model parameters for the 3 equations between groundwater level and SGD (Darcian flow; Darcy–Weisbach Colebrook-White equations; non Darcian flow in a fractal aquifer) and the uncertainty of their fitted parameters (95th confidence interval).

The Darcian flow models and the fractal aquifer model have similar relative uncertainty: 17 % for the fitted parameters of the Darcy model, and 17 % for a and 22 % for b for the Fractal model (Table 1).

By comparison, the uncertainty of the three fitted parameters for the Darcy–Weisbach / Colebrook White equations were much larger (Table 2). The uncertainties for the fitted parameters estimated with the non-linear regression package in R are 550 % of the fitted value for conduit width b and 1300 % of the fitted value for conduit roughness ε. The uncertainty of conduit maximum height y is lower at 60 % (Table 2).

Such large parameter uncertainty for conduit width and roughness led to large prediction and confidence interval for the fitted height discharge relationship using the Darcy–Weisbach / Colebrook White equations. Moreover, the 95th % prediction and confidence interval for discharge using this equation were different when using the higher order Taylor series expansion ($\pm$500 *10^5 m^3/d) than when using the Monte Carlo analysis to estimate it (less than 1 *10^5 m^3/d to 50 *10^5 m^3/d). If we assume that the range of daily flow rate dataset derived from tracer-based estimates is roughly representative of the overall magnitude of natural variability of SGD coming to Kinvarra Bay, such uncertainty seemed unrealistic. By comparison, for the range where data is available, the 95th % prediction and confidence interval were not significantly different for the Taylor series expansion and the Monte Carlo simulations applied when using the fractal model. It is thus possible than the structure of the Darcy–Weisbach / Colebrook White equations (i.e.: the presence of the conditional variable y, coupled with multiple square root terms) is causing a problem during the propagation of uncertainty using higher order Taylor series expansion and Monte Carlo simulation. For this equation, we thus had to use a simplification to assess discharge uncertainty with the Darcy–Weisbach / Colebrook White equations (linearization of uncertainty). We provide in the next paragraphs the results of the different tests we carried out before taking this decision.

First, to assess whether this large parameter uncertainty was an artefact of the method used to assess it within the R package, we tested the effect of the method chosen to calculate parameter uncertainty. This was done using least square fitting within Excel's solver to compare with results from R non-linear solver. We tested parameter fits derived from the two modules applicable in excel for non-linear regression: the GRG solver and the Evolutionary solver (deemed to be less dependent on starting value). For the test, a manual trial and error method was used to set the initial value within the expected range of parameter for karst systems (roughness less than 1, conduit to be expected to be less than 3 m length). The results depended on starting value for the GRG solver and on the parameters applied and on the starting values for the Evolutionary solver (ex: integer optimality). Examples of fitted parameters for the two equations are provided in Table 3. This approach led to fitted parameter values different from the those derived from the R non-linear regression analysis packages, but generally within their range of estimated parameter uncertainty. By themselves these large differences between fits of the equation confirm that many parameters combinations may exist for the Darcy–Weisbach / Colebrook-White equations. In other words, it may exist multiple conduit shapes which may lead to the discharge data derived from tracers mass balances (ex in Fig. 6 and Fig. 7).

Then, we came back to the R script, and tested the effect of reducing the number of fitted parameters on parameter uncertainty (which may occur for example if more field data become available on conduit shapes in the area). Reducing the number of parameters to two (by fixing one of the variable ε or b to a constant during the calculation of uncertainty of the parameter estimate) reduced strongly parameter uncertainty derived from the script of Spiess, (2018). Fixing the conduit width parameter b to 6 m during uncertainty calculation decreased the relative uncertainty for conduit rugosity ε from 1300 % (Table 2) to 93 % (Table 3). Similarly, fixing the conduit rugosity parameter ε to 2 decreased the relative uncertainty for conduit width b from 550 % (Table 2) to 33 % (Table 3). Thus, additional data on conduit width or on conduit rugosity for karst in the area will allow to much better estimate the uncertainty of the other parameters of the Darcy–Weisbach Colebrook-White equations using the higher order Taylor series expansion and Monte Carlo simulation in the propagate R package (Spiess, 2018).

As we do not have at the moment of writing such data on conduit shape or rugosity, but still needed to give some reasonable assessment of uncertainty of the discharge estimates from the Darcy–Weisbach / Colebrook-White equations, we used a simplified method to calculate the 95th % confidence and prediction interval for these fitted equations: The confidence and prediction interval for the fitted Darcy–Weisbach / Colebrook-White equations shown (ex the one shown in Fig. 6 and Fig. 7) are calculated using a linearization approximation (calculation of the uncertainty of this non-linear equation in a similar manner than for a linear regression).

Fitted parameters values for the Darcy–Weisbach / Colebrook-White equations provided in these figures Fig. 6 and Fig. 7 are derived from the non-linear regression analysis in R and should correspond well to a "median" solution. However, the discharge uncertainties provided should be taken with carefulness as this method may not include the full length of uncertainty of the fitted Darcy–Weisbach/Colebrook-White equations. If the linearization approximation does not stand, parameters uncertainty shown in Table 2 for the Darcy–Weisbach / Colebrook-White equations may then be used, but would then lead to very large discharge uncertainties for estimated discharges based on this equation (going well outside of the range of discharge data based on tracer mass balance selected in this work, and of data from Morrissey's hydrogeological model, thus of little use for practical applications for discharge modelling of groundwater flow to Kinvarra Bay).

References

Basu, B., Morrissey, P., Gill, L.W., 2022. Application of Nonlinear Time Series and Machine Learning Algorithms for Forecasting Groundwater Flooding in a Lowland Karst Area. Water Resour. Res. 58, 1–30. https://doi.org/10.1029/2021WR029576.

Bejannin, S., Tamborski, J.J., van Beek, P., Souhaut, M., Stieglitz, T., Radakovitch, O., Claude, C., Conan, P., Pujo-Pay, M., Crispi, O., Le Roy, E., Estournel, C., 2020. Nutrient Fluxes Associated With Submarine Groundwater Discharge From Karstic Coastal Aquifers (Côte Bleue, French Mediterranean Coastline). Front. Environ, Sci, p. 7.

Boycott, T., Bunce, C., Cronin, P., Drew, D., Farrant, A., Hobbs, S., Mullan, G., Self, C., Simms, M., Wilson, L., 2003. Caves of County Clare and South Galway.

Burnett, W.C., Bokuniewicz, H., Huettel, M., Moore, W.S., Taniguchi, M., 2003. Groundwater and pore water inputs to the coastal zone. Biogeochemistry 66, 3–33. https://doi.org/10.1023/B:BIOG.0000006066.21240.53.

Burnett, W.C., Aggarwal, P.K., Aureli, A., Bokuniewicz, H., Cable, J.E., Charette, M.A., Kontar, E., Krupa, S., Kulkarni, K.M., Loveless, A., Moore, W.S., Oberdorfer, J.A., Oliveira, J., Ozyurt, N., Povinec, P., Privitera, A.M.G., Rajar, R., Ramessur, R.T., Scholten, J., Stieglitz, T., Taniguchi, M., Turner, J.V., 2006. Quantifying submarine groundwater discharge in the coastal zone via multiple methods. Sci. Total Environ. 367, 498–543. https://doi.org/10.1016/j.scitotenv.2006.05.009.

Burnett, B., Chanton, J., Christoff, J., Kontar, E., Krupa, S., Lambert, M., Moore, W., O'Rourke, D., Paulsen, R., Smith, C., Smith, L., Taniguchi, M., 2002. Assessing methodologies for measuring groundwater discharge to the Ocean. Eos (washington. DC). 83, 1–5. https://doi.org/10.1029/2002EO000069.

Burnett, W.C., Taniguchi, M., Oberdorfer, J., 2001. Measurement and significance of the direct discharge of groundwater into the coastal zone. J. Sea Res. 46, 109–116. https://doi.org/10.1016/S1385-1101(01)00075-2.

Burnett, W.C., Peterson, R., Moore, W.S., de Oliveira, J., 2008. Radon and radium isotopes as tracers of submarine groundwater discharge - Results from the Ubatuba, Brazil SGD assessment intercomparison. Estuar. Coast. Shelf Sci. 76, 501–511. https://doi.org/10.1016/j.ecss.2007.07.027.

Cave, R.R., Henry, T., 2011. Intertidal and submarine groundwater discharge on the west coast of Ireland. Estuar. Coast. Shelf Sci. 92, 415–423. https://doi.org/10.1016/j.ecss.2011.01.019.

Clare, C., Mcnamara, M.E., 2009. The geology of the Burren region.

Collon, P., Bernasconi, D., Vuilleumier, C., Renard, P., 2017. Statistical metrics for the characterization of karst network geometry and topology. Geomorphology 283, 122–142. https://doi.org/10.1016/j.geomorph.2017.01.034.

Diersch, H.-J.-G., 2009. Discrete feature modelling of flow, mass and heat transport processes using FEFLOW. FEFLOW White Papers I, 151–197.

Drew, D.P., 2008. Hydrogeology of lowland karst in Ireland. Q. J. Eng. Geol. Hydrogeol. 41, 61–72. https://doi.org/10.1144/1470-9236/07-027.

Drew, D., 2003. The hydrology of the Burren and of the Clare and Galway Lowlands., in: Mullan G, Caves of County Clare and South Galway. University of Bristol Spelaeological Society. p. 256.

Dulaiova, H., Burnett, W.C., Chanton, J.P., Moore, W.S., Bokuniewicz, H.J., Charette, M. A., Sholkovitz, E., 2006. Assessment of groundwater discharges into West Neck Bay, New York, via natural tracers. Cont. Shelf Res. 26, 1971–1983. https://doi.org/10.1016/j.csr.2006.07.011.

Duran, L., Gill, L., 2021. Modeling spring flow of an Irish karst catchment using Modflow-USG with CLN. J. Hydrol. 597, 125971.

EPA, 2011. Water Framework Directive Groundwater Monitoring Programme Site information Kinvara Springs.

EPA, 2020. Killiny Borehole water level- EPAHydronet, All data 15min TS and All data DayMean TS [WWW Document]. URL http://www.epa.ie/hydronet/#IE_WE_G_0002_1200_0013 (accessed 1.25.18).

EPA, 2023. EPA Hydronet, Killiny Borehole continuous groundwater levels [WWW Document]. URL http://www.epa.ie/hydronet/#IE_WE_G_0002_1200_0013 (accessed 1.28.23).

Fleury, P., Bakalowicz, M., de Marsily, G., 2007. Submarine springs and coastal karst aquifers: A review. J. Hydrol. 339, 79–92. https://doi.org/10.1016/j.jhydrol.2007.03.009.

Giblin, A.E., Gaines, A.G., 1990. Nitrogen inputs to a marine embayment: the importance of groundwater. Biogeochemistry 10, 309–328. https://doi.org/10.1007/BF00003150.

Gill, L.W., Naughton, O., Johnston, P.M., Basu, B., Ghosh, B., 2013. Characterisation of hydrogeological connections in a lowland karst network using time series analysis of water levels in ephemeral groundwater-fed lakes (turloughs). J. Hydrol. 499, 289–302. https://doi.org/10.1016/j.jhydrol.2013.07.002.

Gill, L.W., Babechuk, M.G., Kamber, B.S., McCormack, T., Murphy, C., 2018. Use of trace and rare earth elements to quantify autogenic and allogenic inputs within a lowland karst network. Appl. Geochemistry 90, 101–114. https://doi.org/10.1016/j.apgeochem.2018.01.001.

Gregory, C., Cave, R.R., Raine, R., Mcdermott, G., O'Flynn, L., 2020. The interaction of retention areas and submarine ground water (SGD) in small bays : implications for phytoplankton growth. Estuar. Coast. Shelf Sci. 106681 https://doi.org/10.1016/j.ecss.2020.106681.

Horlacher, H., Lüdecke, H.-J., 1992. Strömungsberechnung für Rohrsysteme [Current calculation for tube systems]: Ehningen. Springer-Verlag, Germany.

Jeannin, P.Y., 2001. Modeling flow in phreatic and epiphreatic karst conduits in the Hölloch cave (Muotatal, Switzerland). Water Resour. Res. 37, 191–200. https://doi.org/10.1029/2000WR900257.

Kohout, F.A., 1965. The flow of fresh water and salt water in the Biscayne aquifer of the Miami area. Florida. Geol. Surv. Water-Supply Pap. 12, C12–C20.

Kwon, E.Y., Kim, G., Primeau, F., Moore, W.S., Cho, H.-M., DeVries, T., Sarmiento, J.L., Charette, M.A., Cho, Y.-K., 2014. Global estimate of submarine groundwater discharge based on an observationally constrained radium isotope model. Geophys. Res. Lett. 41 (23), 8438–8444.

Luketina, D., 1998. Simple tidal prism models revisited. Estuar. Coast. Shelf Sci. 46, 77–84. https://doi.org/10.1006/ecss.1997.0235.

Maramathas, A.J., Boudouvis, A.G., 2010. A "fractal" modification of Torricelli's formula. Hydrgeol. J. 18 (2), 311–316. https://doi.org/10.1007/s10040-009-0507-2.

Marine Institute, 2020. Galway bay tide data [WWW Document]. Digit. Ocean. URL http://www.digitalocean.ie/Data/DownloadTideData/Galway Port.

McCormack, T., Gill, L.W., Naughton, O., Johnston, P.M., 2014. Quantification of submarine/intertidal groundwater discharge and nutrient loading from a lowland karst catchment. J. Hydrol. 519, 2318–2330. https://doi.org/10.1016/j.jhydrol.2014.09.086.

McCormack, T., Naughton, O., Johnston, P.M., Gill, L.W., 2016. Quantifying the influence of surface water–groundwater interaction on nutrient flux in a lowland karst catchment. Hydrol. Earth Syst. Sci. 20, 2119–2133. https://doi.org/10.5194/hess-20-2119-2016.

Mejías, M., Ballesteros, B.J., Antón-Pacheco, C., Domínguez, J.A., Garcia-Orellana, J., Garcia-Solsona, E., Masqué, P., 2012. Methodological study of submarine groundwater discharge from a karstic aquifer in the Western Mediterranean Sea. J. Hydrol. 464–465, 27–40. https://doi.org/10.1016/j.jhydrol.2012.06.020.

Met Eireann, 2020. Global radiation, temperature and rainfall dataset, taken from the historical dataset for Athenry (2010-) [WWW Document]. URL https://www.met.ie/climate/available-data/historical-data.

Montiel, D., Dimova, N., Andreo, B., Prieto, J., García-Orellana, J., Rodellas, V., 2018. Assessing submarine groundwater discharge (SGD) and nitrate fluxes in highly heterogeneous coastal karst aquifers: Challenges and solutions. J. Hydrol. 557, 222–242. https://doi.org/10.1016/j.jhydrol.2017.12.036.

Moore, W.S., Sarmiento, J.L., Key, R.M., 2008. Submarine groundwater discharge revealed by 228Ra distribution in the upper Atlantic Ocean. Nat. Geosci. 1, 309–311. https://doi.org/10.1038/ngeo183.

Morrissey, P.J., McCormack, T., Naughton, O., Meredith Johnston, P., William Gill, L., 2020. Modelling groundwater flooding in a lowland karst catchment. J. Hydrol. 580, 124361 https://doi.org/10.1016/j.jhydrol.2019.124361.

Mulligan, A.E., Charette, M.A., 2006. Intercomparison of submarine groundwater discharge estimates from a sandy unconfined aquifer. J. Hydrol. 327, 411–425. https://doi.org/10.1016/j.jhydrol.2005.11.056.

Naughton, O., McCormack, T., Drew, D., Gill, L., Johnston, P., Morrissey, P., Regan, S., 2018. The hydrogeology of the Gort Lowlands. Irish J. Earth Sci. 36 (1), 25–44.

Paloc, H., Potie, L., 1974. Etat des connaissances sur les sources littorales et sous-marines.

Paredes, C., Elorza, F.J., 1999. Fractal and multifractal analysis of fractured geological media: Surface-subsurface correlation. Comput. Geosci. 25, 1081–1096. https://doi.org/10.1016/S0098-3004(99)00069-2.

Pongkijvorasin, S., Roumasset, J., Duarte, T.K., Burnett, K., 2010. Renewable resource management with stock externalities: Coastal aquifers and submarine groundwater discharge. Resour. Energy Econ. 32, 277–291. https://doi.org/10.1016/j.reseneeco.2009.09.001.

Povinec, P.P., Aggarwal, P.K. (Eds. ., 2006. Submarine groundwater discharge studies offshore south-eastern Sicily. Cont. Shelf Res. 26, 825–884.

Rocha, C., Wilson, J., Scholten, J., Schubert, M., 2015. Retention and fate of groundwater-borne nitrogen in a coastal bay (Kinvara Bay, Western Ireland) during summer. Biogeochemistry 125, 275–299. https://doi.org/10.1007/s10533-015-0116-1.

Rocha, C., Veiga-Pires, C., Scholten, J., Knoeller, K., Gröcke, D.R., Carvalho, L., Anibal, J., Wilson, J., 2016. Assessing land-ocean connectivity via submarine groundwater discharge (SGD) in the Ria Formosa Lagoon (Portugal): combining radon measurements and stable isotope hydrology. Hydrol. Earth Syst. Sci. 20, 3077–3098. https://doi.org/10.5194/hess-20-3077-2016.

Santos, I.R., Chen, X., Lecher, A.L., Sawyer, A.H., Moosdorf, N., Rodellas, V., Tamborski, J., Cho, H.-M., Dimova, N., Sugimoto, R., Bonaglia, S., Li, H., Hajati, M.-C., Li, L., 2021. Submarine groundwater discharge impacts on coastal nutrient biogeochemistry. Nat. Rev. Earth Environ. 2, 307–323.

Savatier, M., Rocha, C., 2021. Rethinking tracer-based (Ra, Rn, salinity) approaches to estimate point-source submarine groundwater discharge (SGD) into coastal systems. J. Hydrol. 598, 126247.

Savatier, M., 2021. Effect of groundwater-surface interactions on coastal areas hosting aquaculture activities, PhD Thesis.

Schubert, M., Knoeller, K., Rocha, C., Einsiedl, F., 2015. Evaluation and source attribution of freshwater contributions to Kinvarra Bay, Ireland, using 222Rn, EC and stable isotopes as natural indicators. Environ. Monit. Assess. 187, 1–15. https://doi.org/10.1007/s10661-015-4274-3.

Shoemaker, W.B., Kuniansky, E.L., Birk, S., Bauer, S., Swain, E.D., 2008. Documentation of a Conduit Flow Process (CFP) for MODFLOW-2005 A product of the Ground-Water Resources Program. U.S. Geol. Surv Techniques 50.

Smith, A.M., Cave, R.R., 2012. Influence of fresh water, nutrients and DOC in two submarine-groundwater-fed estuaries on the west of Ireland. Sci. Total Environ. 438, 260–270. https://doi.org/10.1016/j.scitotenv.2012.07.094.

Smith, L., Zawadzki, W., 2003. A hydrogeologic model of submarine groundwater discharge: Florida intercomparison experiment. Biogeochemistry 66, 95–110. https://doi.org/10.1023/B:BIOG.0000006108.80520.c9.

Spiess, A.-N., 2018. propagate R package, Propagation of uncertainty using higher-order Taylor expansion and Monte Carlo simulation, Available on CRAN repository, Version: 1.0-6.

Taniguchi, M., Dulai, H., Burnett, K.M., Santos, I.R., Sugimoto, R., Stieglitz, T., Kim, G., Moosdorf, N., 2019. Submarine Groundwater Discharge : Updates on Its Measurement Techniques, Geophysical Drivers, Magnitudes, and Effects. Front. Environ. Sci. 7, 1–26. https://doi.org/10.3389/fenvs.2019.00141.

Williams, P.W., 1974. Hydrogeological setting of the Waikoropupu springs 35.

Yu, B., Cheng, P., 2002. A fractal permeability model for bi-dispersed porous media. Int. J. Heat Mass Transf. 45, 2983–2993. https://doi.org/10.1016/S0017-9310(02)00014-5.